Redescription of Arganasaurus (Metoposaurus) azerouali (Dutuit) comb. nov. from the Upper Triassic of the Argana Basin (Morocco), and the first phylogenetic analysis of the Metoposauridae (Amphibia, Temnospondyli)

Valentin Buffa, Nour-Eddine Jalil, J.-Sébastien Steyer

REDESCRIPTION OF *ARGANASAURUS* (*METOPOSAURUS) AZEROUALI* (DUTUIT) COMB. NOV. FROM THE LATE TRIASSIC OF THE ARGANA BASIN (MOROCCO), AND THE FIRST PHYLOGENETIC ANALYSIS OF THE METOPOSAURIDAE (AMPHIBIA, TEMNOSPONDYLI)

by VALENTIN BUFFA*[1], NOUR-EDDINE JALIL[1,2] *and* J.-SEBASTIEN STEYER[1]

[1]Centre de Recherche sur la paléobiodiversité et les paléoenvironnements, UMR 7207 CNRS-MNHN-UPMC, Muséum national d'Histoire naturelle, CP38, 8 rue Buffon, 75005 Paris ; e-mails: valentin.buffa@edu.mnhn.fr, nour-eddine.jalil@mnhn.fr, jean-sebastien.steyer@mnhn.fr

[2]BioDEcos Département de géologie, Faculté des Sciences Semlalia, Université Cadi Ayyad, Marrakech, Maroc

*Corresponding author

Abstract: A systematic revision of the temnospondyl "*Metoposaurus" azerouali* Dutuit from the Late Triassic of the Argana Basin (Western High Atlas, Morocco) is presented. The type material is redescribed in detail, and a preliminary phylogenetic analysis - the first one dealing with all metoposaurid species - is also conducted in order to test its position within the Metoposauridae. Our analysis places "*Metoposaurus" azerouali* as sister-taxon to *Arganasaurus lyazidi* in a robust clade supported by two unambiguous synapomorphies (buldge-like tabular horn and exoccipital process visible in dorsal view) and two ambiguous synapomorphies (cultriform process of uniform width and subtriangular posterior Meckelian fenestra). We therefore propose the new combination *Arganasaurus azerouali* comb. nov. for the species "*M.*" *azerouali*. Our analysis also confirms that the central Laurasian genus *Metoposaurus* is monophyletic but not the genus *Koskinonodon* which deserves its own systematic revision. By consequent, the Late Triassic rich vertebrate fauna from the Argana Basin comprises the metoposauroid *Almasaurus habazzi*, the basal metoposaurid *Dutuitosaurus ouazzoui*, and the genus *Arganasaurus* which is represented by the type species *A. lyazidi* and *A. azerouali* comb. nov. Combined with the stratigraphic and geographic occurrences of the taxa, our phylogenetic analysis suggests that metoposaurids may have appeared during the Longobardian (late Ladinian) in central Pangea. Their diversification may be linked to the Carnian Pluvial Episode. At least, their extinction may have occurred during the Rhaetian because of the aridification of the climate and/or competition with amniotes.

Keywords: phylogenetic analysis, Metoposauridae, diversification, Carnian Pluvial Episode, temnospondyl, Morocco.

The Argana Basin, also called the Argana Corridor (Western High Atlas, Morocco), provides a series of continental deposits spanning from the Middle-Late Permian to the early Jurassic. Since the 1960s, this basin has yielded numerous fossils that document a key period in the

evolutionary history of terrestrial vertebrates, including the Permo-Triassic mass extinction (Khaldoune *et al.* 2017).

Among the Triassic amphibians recovered from the Argana Basin, three species of metoposaurids are known: *Dutuitosaurus ouazzoui* (Dutuit, 1976)*, Arganasaurus lyazidi* (Dutuit, 1976) and "*Metoposaurus" azerouali* Dutuit, 1976. The latter has been described briefly in French by Dutuit (1976, p. 165-176) and its systematic status is controversial as it has been considered as a *nomen dubium* by Hunt (1993) but a valid taxon by Schoch and Milner (2000).

The family Metoposauridae Watson, 1919 includes temnospondyl amphibians which occupied freshwater predatory niches during the Late Triassic, especially between the middle Carnian and the Norian (Hunt 1993; Schoch and Milner 2000; Sulej 2002; Brusatte *et al.* 2015). Metoposaurids are found in low palaeolatitude deposits in Europe, India, Morocco and North America (Case 1922, 1931; Dutuit 1976; Hunt 1993; Sengupta 2002; Sulej 2002; Brusatte *et al.* 2015) and presumably in Algeria, France and Madagascar (Schoch and Milner 2000). The position of the Metoposauridae within temnospondyls has been an ongoing debate for decades, but the current consensus considers them as trematosaurian stereospondyls (Schoch and Milner 2000; Yates and Warren 2000; Damiani and Yates 2003; Schoch 2008, 2011, 2013).

Several phylogenetic studies involving metoposaurids have been done (Hunt 1993; Steyer 2002; Ruta *et al.* 2007; Sulej 2007; Schoch 2008, 2011, 2013; McHugh 2012) but the only computer-based phylogenetical analyses to date were conducted on temnospondyls or stereospondyls as a whole and did not take into account all metoposaurid species. This study provides a systematic revision of the species "*Metoposaurus" azerouali* Dutuit, 1976 and the first preliminary phylogenetic analysis of the family Metoposauridae.

Institutional abbreviation. BMNH, British Museum of Natural History, London; MNHN, Muséum national d'Histoire naturelle, Paris.

SYSTEMATIC PALAEONTOLOGY

Order TEMNOSPONDYLI Zittel, 1888

Suborder STEREOSPONDYLI Zittel, 1888

Family METOPOSAURIDAE Watson, 1919

Phylogenetic definition. Node-based clade including the last common ancestor of *Dutuitosaurus ouazzoui* and *Metoposaurus diagnosticus* (Meyer, 1842) and all of its descendants (see analysis below).

Diagnosis (modified from Sulej 2007). Large oval and widely separated orbits in the anterior half of the skull; parasphenoid central depression; broad cultriform process; absence of cultriform process keel; quadrate excluded from squamosal by quadratojugal; quadrate condyle subtriangular in ventral view; paraquadrate foramen present; deep and rounded sinus pterygoidei below the oblique crest on the posterior side of the ascending ramus of the pterygoid; mandibular dentition strictly on the dentary; prearticular not anteriorly positioned to the posterior coronoid; articular extending posteriorly between the surangular and the prearticular along the dorsal surface of the retroarticular process; parapophysis on two neighboring intercentra of presacral and sacral vertebra; neural spine dorsally extended in posterior trunk or tail; clavicular blade indentation; clavicular contact above the interclavicle; unusually large manus and pes; concave anterior margin of the ilium shaft; main axes of the proximal and distal heads of the femur set to each other at 90°.

Content. The type species *Metoposaurus diagnosticus* from Germany; *Metoposaurus krasiejowensis* (Sulej, 2002) from Poland (we followed Brusatte *et al.* 2015 in considering the subspecies "*M. diagnosticus krasiejowensis*" Sulej, 2002 as the species *M. krasiejowensis*); *Metoposaurus algarvensis* Brusatte, Butler, Mateus and Steyer, 2015 from Portugal; *Koskinonodon perfectus* (Case, 1922) and *Koskinonodon bakeri* (Case, 1931) (following the generic attribution of Sulej 2007 and Brusatte *et al.* 2015) from North America; *Koskinonodon maleriensis* (Chowdhury, 1965) from India (following the generic attribution of Sengupta 2002, 2003 and the remarks of Brusatte *et al.* 2015); *Dutuitosaurus ouazzoui*, *Arganasaurus lyazidi* and "*Metoposaurus" azerouali* from Morocco.

Remarks. In his diagnosis of the Metoposauridae, Sulej (2007) also added large external nostrils and an exoccipital-pterygoid suture perpendicular to the skull axis in ventral view. However, as these characters are also shared with *Callistomordax kugleri* Schoch, 2008, sister-taxon to the Metoposauridae in our analysis (see below), we consider them as no longer valid for this diagnosis.

In his revision, Hunt (1993) discriminated the genera *Koskinonodon* (Case, 1922) and *Metoposaurus* Lydekker, 1890 on the basis of the lacrimal entering or not the orbit (respectively). However, as recent works showed that the lacrimal does enter the orbit in the genus *Metoposaurus* (Sulej 2002, 2007; Brusatte *et al.* 2015), this discrimination is no longer valid. While the diagnosis of the genus *Metoposaurus* has been amended (Sulej 2002, 2007; Brusatte *et al.* 2015), *Koskinonodon* still needs a systematic revision, which is out of the scope of this paper.

Apachesaurus gregorii Hunt, 1993 from the Norian of North America has recently been considered as a juvenile form of a large metoposaurid, potentially *Koskinonodon perfectus* (Gee and Parker 2017, 2018a, b; Gee *et al.* 2017). To test this hypothesis, we decided to keep the species *A. gregorii* in our phylogenetic analysis.

Several Metoposaurid taxa from other localities have been erected but they are of disputed validity: "*Metoposaurus santaecrucis*" Koken, 1913 from the Triassic of Italy and Switzerland has been synonymized with *Metoposaurus diagnosticus* by Sulej (2002); "*Metoposaurus heimi*" Kuhn, 1932 from southeastern Germany is based on a lost holotype (see Schoch and Milner 2000); "*Metoposaurus hoffmani*" Dutuit, 1978 from the Late Triassic of Madagascar is not valid according to Hunt (1993) and Schoch and Milner (2000). Fragments of presumably metoposaurids have also been mentioned in the lower Keuper and Norian of France (Corroy 1928; Cuny and Ramboer 1991) and in the Late Triassic of Algeria (Lehman 1971).

Genus ARGANASAURUS Hunt, 1993

Type Species. Arganasaurus lyazidi (Dutuit, 1976)

Diagnosis (modified from Hunt 1993). Subtriangular squamosal; shallow otic notch with buldge-like tabular horn; postero-ventrally angled occipital surface, visible in dorsal view (see characters 31 and 35, Buffa *et al.* 2018, appendix 1).

Content. The type species *Arganasaurus lyazidi* and *Arganasaurus azerouali* comb. nov., both from the Carnian of the Argana Basin (Locality XIX, and XV and VII bis respectively, upper part of the "T5 Unit" *sensu* Dutuit 1976).

Remarks. The diagnosis of the genus *Arganasaurus* was previously defined by monotypy as that of *Arganasaurus lyazidi*. We add three new diagnostic characters for the genus *Arganasaurus* (see phylogenetic analysis below) and consider the diagnostic characters of Hunt (1993) as diagnostic characters of *Arganasaurus lyazidi*. The first description of the pectoral girdle elements of the type species *Arganasaurus lyazidi* (used to code character states for characters 61 and 62) is provided on Appendix 1 (Buffa *et al.* 2018).

ARGANASAURUS (METOPOSAURUS) AZEROUALI (DUTUIT, 1976) COMB. NOV.

Synonymy. Metoposaurus azerouali Dutuit, 1976 (pl. 35-43; figs 72-77; p. 165-177).

Holotype. MNHN.F.ARG 5, a relatively well preserved and slightly deformed skull (39.5 cm long, 35.6 cm wide and 9.1 cm high) described and figured by Dutuit (1976, pl. 35, 36, 41E; figs 72-74; p. 165, 168, 169, 171, 172, 176).

Paratypes. MNHN.F.ARG 9-1-3: two sub-complete clavicles with the corresponding articulated interclavicle described and figured by Dutuit (1976, pl. 41C, p. 172, 173).

Type locality and horizon. Locality XV near the village Imziln, northern part of the Argana Basin (Western Atlas, Morocco); Upper section of the "T5 Unit" (*sensu* Dutuit 1976), Irohalène Member, Timezgadiouine Formation, Carnian, Late Triassic.

Referred material. MNHN.F.ARG 1: right clavicle portion; MNHN.F.ARG 2: incomplete interclavicle; MNHN.F.ARG 3: complete right hemi-mandible; MNHN.F.ARG 4: subcomplete left hemi-mandible; MNHN.F.ARG 8: left clavicle with missing ornamentation; MNHN.F.AZA 14: interclavicle portion; MNHN.F.AZA 28: subcomplete left clavicle; MNHN.F.TAL 12: right skull portion; MNHN.F.TAL 16: interclavicle portion; MNHN.F.TAL 17: left skull portion; MNHN.F.TAL 27: right clavicle portion; MNHN.F.TAL 93: right clavicle portion.

Diagnosis (modified from Dutuit 1976; Schoch and Milner 2000). Arganasaurus azerouali comb. nov. differs from the type species *Arganasaurus lyazidi* by possessing the following autapomorphies (see characters 1, 6, 9, 28, 30 and 50, Buffa *et al.* 2018, appendix 1): very thick and massive cranial and postcranial bones; maxilla entering the orbital margin (shared with *Dutuitosaurus*); lacrimal entering the orbit margin (shared with *Metoposaurus* and

Koskinonodon perfectus); ornamentation with very few ridges; relatively poorly developed lateral line system (except on the hemi-mandibles); orbits in the anterior quarter of the interpterygoid fenestrae (shared with *Koskinonodon perfectus*); cultriform process very broad but narrowing anteriorly; no splenial contribution to the symphysis (shared with *Dutuitosaurus*); subtriangular posterior Meckelian fenestra; very large pitted zone in the ornamentation of the pectoral girdle elements (shared with *Dutuitosaurus ouazzoui*, *Apachesaurus gregorii*, *Koskinonodon bakeri* and *Koskinonodon perfectus*) .

Remarks. We followed the status of the type material originally given by Dutuit (1976) *contra* Hunt (1993) and Khaldoune *et al.* (2017) in virtue of the International Code of Zoological Nomenclature. Hunt (1993) designated the skull MNHN.F.ARG 5 and the articulated clavicles and interclavicle MNHN.F.ARG 9-1-3 as lectotype and paralectotypes respectively. Khaldoune *et al.* (2017) later designated the same skull as the lectotype with the hemi-mandibles MNHN.F.ARG 3 and MNHN.F.ARG 4 as paralectotypes. However, the skull MNHN.F.ARG 5 and the clavicles and interclavicle MNHN.F.ARG 9-1-3 had already been designated as holotype and paratypes respectively by Dutuit (1976) in his original description. No type status was given to the hemi-mandibles MNHN.F.ARG 3 and MNHN.F.ARG 4.

Schoch and Milner (2000) considered the large size of *A. azerouali* comb. nov. as a diagnostic character. However, as size is subjected to many biases, we follow Hunt (1993) and Gee and Parker (2017) for whom it cannot be considered a diagnostic character for metoposaurids. Schoch and Milner (2000) also proposed the small teeth in the palatal series of *A. azerouali* comb. nov. as a diagnostic character, but we do not consider the teeth of MNHN.F.ARG 5 “small” compared to that of other metoposaurids.

REDESCRIPTION

Cranial general features

The holotype MNHN.F.ARG 5 (Fig. 1A) is relatively complete but slightly deformed, especially on its palatal surface. The skull is relatively large compared to other metoposaurids, and the bones are thick (the jugal is 1.0 cm high), rendering the skull massive.

The skull is typically metoposaurian in shape: dorsoventrally compressed, broad posteriorly and gradually narrowing anteriorly, and with orbits in anterior position. The nares, visible on MNHN.F.TAL 12 and MNHN.F.TAL 17 (Fig. 2), are ovoid and located very anteriorly. In MNHN.F.ARG 5 (Fig. 1A), they are not visible in dorsal view because they are marginal. The orbits are laterally positioned, widely separated and situated in the anterior half of the skull. The pineal foramen is situated in the middle of the posterior half of the skull, and is unusually large (2 cm in diameter). The otic notches are relatively shallow.

The dermal ornamentation of the cranial bones consists in deep alveoli only, hereby called ‘pits’ following the usual term for metoposaurids (Hunt 1993; Schoch and Milner 2000; Sulej 2002, 2007; Brusatte *et al.* 2015). The grooves, which indicate an active growth zone (Moodie 1908; Dutuit 1976; Steyer 2000; Sulej 2007), are not present here, even between the nares and the orbits or between the orbits and the pineal foramen as is usually the case in metoposaurids (Dutuit 1976; Steyer 2000; Sulej 2007). Most of the cranial sutures are very open and well visible. Adding to the unusually large pineal foramen, these characters suggest a juvenile or a sub-adult growth stage (Boy 1974; Steyer 2000).

Skull Roof

The premaxilla, incomplete on MNHN.F.TAL 12 and MNHN.F.TAL 17 (Fig. 2), forms the most anterior part of the skull and contacts the nasal posteromedially, the nares posteriorly and the maxilla laterally.

The nasal is subpolygonal, medially positioned and large, making up most of the skull width anteriorly. It contacts the premaxilla anteromedially, the frontal posteromedially, the prefrontal posterolaterally and the lacrimal and maxilla laterally.

The maxilla is the longest bone on the skull roof and forms the anterolateral margin of the skull. It does not bear any ornamentation. It contacts the nasal and premaxilla anteriorly, the lacrimal medially and the jugal posteriorly. It also enters the orbit posteromedially (Fig. 1B). The maxilla-jugal suture indeed enters the orbit in its posterior third, which leaves the medial third in contact with the maxilla. This is also the case in *D. ouazzoui* (Dutuit 1976). The left maxilla of MNHNF.ARG 5 bears an incomplete row of six teeth on its ventral surface (Fig. 3).

The lacrimal is elongate, almost as long as the preorbital region, contrary to that of *M. diagosticus*, *K. perfectus* and *A. gregorii* where it is compact (Schoch and Milner 2000; Spielmann and Lucas 2012; Lucas *et al.* 2016). In *A. azerouali* comb. nov., it contacts the nasal anteromedially, contrary to that of *K. perfectus* and *A. gregorii* (Spielmann and Lucas 2012; Lucas *et al.* 2016) where this contact is absent. It also contacts the prefrontal medially. On MNHN.F.ARG 5, MNHN.F.TAL 12 and MNHN.F.TAL 17, the lacrimal contacts the anterior margin of the orbit (Figs 1B, 2). This is also found in *Metoposaurus*, *K. perfectus* and *K. maleriensis* (Sulej 2007; Brusatte *et al.* 2015; Lucas *et al.* 2016).

The prefrontal is large (about half long and third wide of the whole preorbital region) and subrectangular. It contacts the nasal anteriorly and the lacrimal anterolaterally (Fig. 1B), contrary to that of *K. perfectus* and *A. gregorii* where it contacts the nasal and maxilla anteriorly (Spielmann and Lucas 2012; Lucas *et al.* 2016). In *A. azerouali* comb. nov., it also contacts the frontal medially and the orbit and postfrontal posteriorly. The prefrontal-postfrontal suture is anterolaterally oblique, contrary to *M. krasiejowensis* (Brusatte *et al.* 2015), thus the contribution of the prefrontal to the orbit is reduced, contrary to *K. perfectus* and *A. gregorii*

(Spielmann and Lucas 2012; Lucas *et al.* 2016). The prefrontal does not contact the jugal, contrary to *K. bakeri*, *A. gregorii* and *A. lyazidi*.

The frontal is subrectangular, elongate (more than the third of the skull length) and tapered to a point posteriorly. It contacts the nasal anteriorly, the prefrontal anterolaterally, the postfrontal posterolaterally and the parietal posteriorly.

The postfrontal is elongate and slightly angled lateromedially, about half the length of the postorbital region. It broadly contacts the orbit (Fig. 1B), contrary to *K. perfectus* and *A. gregorii* where this contact is reduced (Spielmann and Lucas 2012; Lucas *et al.* 2016). It also contacts the prefrontal anteriorly, the frontal medially, the postorbital laterally and the supratemporal (at least on the right side of MNHN.F.ARG 5) and parietal posteriorly.

The postorbital is elongate, about half the length of the postorbital region. It contacts the orbit anteriorly, the postfrontal medially, the jugal laterally, the squamosal posterolaterally and the supratemporal posteriorly.

The jugal is elongate (more than the half length of the postorbital region) and laterally positioned on the skull roof. Its anterior margin is posterior to the anterior orbital margin (Fig. 1B), contrary to *M. diagnosticus*, *M. krasiejowensis*, *M. algarvensis* and *K. maleriensis* where it ends anteriorly to the anterior orbital margin, and to *A. gregorii* and *A. lyazidi* where it is leveled with the anterior orbital margin. In *A. azerouali* comb. nov., it forms the anterolateral margin of the posterior half of the skull. It borders the orbit anteriorly, and contacts the maxilla laterally, the postorbital medially and the squamosal posteriorly.

The parietal is subrectangular, tapered to a point anteriorly. It extends from the midline of the postorbital-prepineal region to the midline of the postpineal region. It contacts the frontal and postfrontal anteriorly, the supratemporal laterally and the postparietal anteriorly. It is pierced medially by the pineal foramen in its posterior half.

Sulej (2002) discriminated *M. diagnosticus* and *M. krasiejowensis* based on the prepineal length of the parietal (proportionnally long and short respectively) and the "expansion angle" of the parietals (i.e. the angle between the left and right parietal-supratemporal sutures; narrow and wide respectively). Brusatte *et al.* (2015) described *M. algarvensis* as having a prepineal length similar to that of *M. krasiejowensis* and an expansion angle similar to that of *M. diagnosticus*. The expansion angle cannot be measured on the holotype of *A. azerouali* comb. nov. as the left and right parietal-supratemporal sutures are almost parallel. The prepineal length is different on the left and right parietals (10.2 cm and 8.6 cm respectively) but both are similar to the length of *M diagnosticus*.

The postparietal is small and subrectangular. It contacts the parietal anteriorly, the supratemporal anterolaterally and the tabular posterolaterally. Its posterior margin is straight medially and concave laterally. It forms the medial part of the posterior margin of the skull table.

The supratemporal is subrectangular and elongated (almost the half length of the postorbital region). It contacts the postfrontal (at least on the right side of MNHN.F.ARG 5) and postorbital anteriorly, the parietal medially, the postparietal posteromedially, the squamosal laterally and the tabular posteriorly.

The tabular is small and subrectangular. It contacts the postparietal anteromedially and the supratemporal anterolaterally. Its posterior margin is strongly convex. It forms the posterolateral margin of the skull table, and the medial margin of the otic notch. It bears a reduced tabular horn compared to other metoposaurids.

The squamosal is subtriangular and pointed anteriorly (Fig. 1B) as in *A. lyazidi* (it is polygonal in the other metoposaurids, Dutuit 1976; Spielmann and Lucas 2012; Lucas *et al.* 2016). Brusatte *et al.* (2015) described *M. algarvensis* as having a subtriangular squamosal but

its medial margin is curved, contrary to the straight medial margin in both *Arganasaurus* species. In *A. azerouali* comb. nov., the squamosal extends on almost two thirds of the postorbital length. It contacts the postorbital anteromedially, the jugal anterolaterally, the supratemporal medially and the quadratojugal laterally. The posterior margin of the squamosal is concave medially and straight laterally. It forms the third quarter of the posterior skull margin and the anterior and lateral margins of the otic notch.

The quadratojugal is a relatively small, with a length similar to that of the postpineal region. Its lateral margin is convex and forms the most posterolateral margin of the skull. It contacts the squamosal along the medial margin.

The depth of the otic notches and the development of the tabular horns have been used to differentiate the Metoposauridae genera (Gregory 1980; Hunt 1993; Schoch and Milner 2000). Compared with the other metoposaurids, the otic notches of *A. azerouali* comb. nov. are shallow (Figs 1, 4) and their tabular horns are buldge-like and poorly developed (0.9 cm), contrary to the posterolaterally projecting tabular horn of other metoposaurids. These otic notches are similar in shape to that of *A. lyazidi*. *A. gregorii* has extremely shallow otic notches and no tabular horn – an argument to state that *A. gregorii* is a juvenile metoposaurid (Gee and Parker 2017, 2018a, b; Gee *et al.* 2017). Here, the otic notches of *A. azerouali* comb. nov. and *A. lyazidi* are not different in relative size (of "intermediate" depth between the well-developed otic notches of most metoposaurids and the extremely shallow ones of *A. gregorii* according to Hunt 1993), that is why we consider the shallow otic notches and buldge-like tabular horn of *A. azerouali* comb. nov. and *A. lyazidi* as diagnostic and not related to ontogeny.

The postorbital canals begin on the posterolateral margin of the squamosal, farther back than those of *D. ouazzoui* (Dutuit 1976) but similar to those of *K. perfectus* (Case 1922; Schoch and Milner 2000; Lucas *et al.* 2016). The canal on the right side of MNHN.F.ARG 5 runs along the lateral margin of the squamosal and the left one along the medial margin of the

quadratojugal. They extend anteriorly on the posterior half of the jugal and form a convex loop on the posterior half of the postorbital. They end posteriorly on the supratemporal, at the same level than the pineal foramen. The width of the postorbital canals progressively increases, from 0.4 cm on the squamosal to 1.3 cm on the supratemporal.

The infraorbital canal is visible only on MNHN.F.TAL 17 (Fig. 2). It is about 0.7 cm wide. It starts on the maxilla, gently curves on the lacrimal between the nare and the orbit, and continues laterally on the jugal before joining the postorbital canal where the latter forms a convex loop.

The supraorbital canal is poorly developed because it forms a punctuated canal rather than a continuous groove (Fig. 1). It is about 2 cm wide. It starts on the premaxilla anteriorly (as seen only on MNHN.F.TAL 12, Fig. 2), curves on the nasal and lacrimal between the nare and the orbit (contrary to *K perfectus* and *A. gregorii* where it passes medially to the lacrimal, Spielmann and Lucas 2012; Lucas *et al.* 2016), runs medially toward the orbit on the prefrontal, frontal, postfrontal and postorbital, where it joins the postorbital canal in its convex loop.

Palate

Dutuit (1976: 169) gave a brief description of the palate. The palate of the holotype is more deformed and less well-preserved than the skull roof, especially in its anterior portion (Fig. 3A).

The interpterygoid fenestrae are extremely large and somewhat teardrop-shaped, with an anteriorly tapered end, as in *M. algarvensis* (Brusatte *et al.* 2015). They cover most of the anterior half of the palatal surface and are separated by a broad cultriform process of the parasphenoid. The subtemporal fenestrae are large (more than two thirds of the palatal length) and subtriangular.

In palatal view, the orbits are located in a very anterior position within the interpterygoid fenestrae: they occupy the anteriormost quarter of the latter. This is not the case in other metoposaurids (except in *K. perfectus*, Lucas *et al.* 2016) in which the orbits are located in the second anterior quarter of the interpterygoid fenestrae. These very anterior orbits of *A. azerouali* comb. nov. do not seem linked to a juvenile growth stage because juvenile individuals of *D. ouazzoui* have relatively posterior orbits within the interpterygoid fenestrae (Dutuit 1976).

The maxilla bears a row of small teeth (0.4 to 0.5 cm in diameter), of which six are visible on MNHN.F.ARG 5 (Fig. 3). A parallel row of teeth (0.2 to 0.8 cm in diameter) extends on the palatine and ectopterygoid: eight teeth are visible on the left maxilla and 14 on the right one, preceded by a large anterior tusk of 1.6 cm wide. No alveoli could be observed, but this may be due to the preservation.

The choanae, of approximately 3.6 x 2.2 cm, are relatively large compared with the skull size (their maximum length is close to that of the orbit). Both choanae are ovoid-elongate in shape, as in *M. krasiejowensis*, but the right one looks slightly more elongate than the left one in MNHN.F.ARG 5 (Fig. 3). They are located very posteriorly in comparison with other metoposaurids: their posterior border is located at the level of the anterior margin of the interpterygoid fenestrae. The inter-choanal distance (of approximately 12 cm) is large, approximately one third of the maximum skull width, as in *M. algarvensis*.

The vomerian plateau covers a large part of the anterior palate. Both vomers are partly separated by an elongate extension of the cultriform process of the parasphenoid. As the anterior portion of the palate is weathered, it is difficult to observe the sutures of the vomer with the premaxilla and maxilla. However, the suture of the vomer with the palatine is visible on the right side of MNHN.F.ARG 5 (Fig. 3): it reaches the posterior tip of the choana.

The palatine is elongate and located just posteriorly to the choana. The left palatine of MNHN.F.ARG 5 bears a palatal tusk of 1.6 cm in diameter (Fig. 3). Because of its poor preservation state, the suture of the palatine with the ectopterygoid is unfortunately not visible.

The parasphenoid has a peculiar shape (Fig. 3): the parasphenoid plate, which forms the medial part of the palate posterior to the interpterygoid fenestrae, is very elongate and subrectangular. It extends into a very long and wide cultriform process anteriorly, separating the interpterygoid fenestrae. This cultriform process is tapered to a point anteriorly, also separating partly the vomers: its anterior extension is very anteriorly located, at the level of the choanae, as is the case in *M. krasiejowensis*. The dorsal surface (i.e. the surface between the bone and the skull roof) of the cultriform process forms a gutter in its medial third, as described for *D. ouazzoui* (Dutuit 1976: fig. 4). The posterior quarter of the cultriform process is significantly thinner, which differentiates *A. azerouali* from other metoposaurids and is thus considered diagnostic (Case 1922; Dutuit 1976; Hunt 1993; Sengupta 2002; Sulej 2007; Brusatte *et al.* 2015; Lucas *et al.* 2016). The ventral ornamentation of the parasphenoid is composed of small subtle pits radiating from the center of the parasphenoid plate to its periphery. It extends on the cultriform process on MNHN.F.ARG 5, contrary to all other metoposaurids except *K. perfectus*. The T-shaped crista muscularis is visible in the posterior half of the parasphenoid plate of MHNH.F.ARG 5 but its medial ridge (i.e. the vertical bar of the 'T') is damaged (Fig. 3). The horizontal ridges (i.e. the two ridges forming the horizontal bar of the 'T') are around 2.5 cm long each and do not extend on the pterygoid.

The ectopterygoid is located medially to the posterior portion of the maxilla and anteriorly to the palatal ramus of the pterygoid. It is elongate and bears a tooth row visible on MNHN.F.ARG 5, with the diameter of the tooth basis progressively reducing posteriorly. However the ectopterygoid is not a very narrow bone (as seen in *M. krasiejowensis*): it ends posteriorly drawing a substantial margin with the subtemporal fenestra, as in *M. algarvensis*.

The pterygoid takes most of the posterior half of the palate. It has a typical triradiate shape in palatal view. Its corpus is subrectangular and contacts the parasphenoid plate in a slightly jagged anteroposteriorly oriented margin. The pterygoid-parasphenoid suture is very elongate, a typical stereospondyl character (e.g., Yates and Warren 2000). The pterygoid corpus extends anterolaterally into the palatal ramus, posterolaterally into the quadrate ramus and posteromedially into the basipterygoid ramus. The palatine ramus is the longest ramus, separating the interpterygoid fenestra and the subtemporal fenestra, and contacting the ectopterygoid in its anterior end. The quadrate ramus is very posteriorly widened and forms a third of the palatal posterior margin. The basipterygoid ramus, visible on the right side of MNHN.F.ARG 5, is short. The corpus and palatal rami of the pterygoid are slightly ornamented, with small subtle pits. The palatine ramus bears a posterolateral flange, as in most metoposaurids.

The quadrate is visible in palatal and occipital view. It consists of a large (proportionally to the skull size) and bulged bone located at the extremity of the quadrate ramus of the pterygoid, posteriorly to the subtemporal fenestra. It is robust and massive, as is the case in *M. krasiejowensis*. Its ventral surface is weathered, especially in its contact zone with the pterygoid, but an oblique crest is visible. Unfortunately its preservation state does not allow a more precise description.

Occiput

The occiput is well preserved, 35.6 cm wide and 9.1 cm high (Fig. 4). These measurements are more similar to those of *M. krasiejowensis* than of *M. algarvensis*. In *A. azerouali* comb. nov., the dorsal margin of the occiput is slightly convex, as in *D. ouazzoui* (Dutuit 1976). The occiput projects posteriorly, similar to all other metoposaurids except *A.*

gregorii (Hunt 1993; Spielmann and Lucas 2012). The occipital surface is slightly inclined posteroventrally, making it partially visible in dorsal view, as is the case in *A. lyazidi*. The articular condyles are slightly more ventral than the occipital condyle.

The squamosal is subrectangular and convex in occipital view. It bears the otic notches (described above) and the crista falciformis, and contacts the paraquadrate foramen laterally. The crista falciformis is present as a modest ridge, as in all metoposaurids.

The pterygoid is the largest bone in occipital view but the less extended posteriorly. Its ventral margin is relatively straight and makes a third of the occipital width. It borders the paraquadrate foramen and bears the otic flange (a posteriorly projecting ridge separating the squamosal and the pterygoid on the occipital surface) similar to all metoposaurids.

The exoccipitals form the medial part of the ventral margin of the occiput. They contact the foramen magnum dorsally and bear the occipital condyles. These condyles are 3.6 cm wide and subcircular, as in *M. krasiejowensis* (those of *M. algarvensis* look relatively flat but this could be due to the preservation state). In *A. azerouali* comb. nov., these condyles are well-spaced along the occipital width (around 3 cm), more than those of *D. ouazzoui* or *M. krasiejowensis*. The ascending branch of the exoccipital forms the occipital pillar (4.3 to 4.9 cm high) which bears the posttemporal foramen (see below) and borders the foramen magnum. This occipital pillar widens dorsally (around 2.3 cm above the condyles and around 4.8 cm near the skull dorsal margin).

The foramen magnum is 6.4 cm high and occupies most of the medial margin of the occiput (Fig. 4). Its left margin is slightly compressed medially, but the foramen is globally keyhole-shaped, similar to all metoposaurids except *A. gregorii* which has a subtriangular foramen magnum (Spielmann and Lucas 2012). In *A. azerouali* comb. nov., the dorsal portion of this foramen is relatively high, as in *M. algarvensis*, but its ventral portion is still deeper.

The paraquadrate foramen is very large and bordered by the squamosal dorsally, the quadratojugal laterally, the quadrate ventrally and the pterygoid medially (Fig. 4). It is subtriangular and very widened transversally (up to 2.7 cm wide), wider than that of *D. ouazzoui* (Dutuit 1976). This differentiates *A. azerouali* comb. nov. from *K. perfectus* and *A. gregorii* (Spielmann and Lucas 2012) where the paraquadrate foramen is small. No paraquadrate accessory foramen has been found on this skull, contrary to *M. diagnosticus* or *A. gregorii* (Speilmann and Lucas 2012).

The posttemporal foramen is located just above the occipital pillar. It is very small and subcircular (1.5 cm in diameter), similar to all metoposaurids except *A. gregorii*, *A. lyazidi*, *D. ouazzoui* and *K. perfectus* in which the posttemporal foramen is small and polygonal (Fig. 4).

Mandible

This study is based on the two associated (but not articulated) hemi-mandibles (MNHN.F.ARG 3, Fig. 5, MNHN.F.ARG 4, Dutuit 1976, pl. 37C, 38C, 39A, B, E-G) belonging to the above-described skull MNHN.F.ARG 5. The right hemi-mandible is complete. As for the skull, the impressive dimensions of these hemi-mandibles were also noted by Dutuit (1976: 170). The right hemi-mandible is 46.1 cm long, 6.9 to 2.9 wide (narrowing in the medial third) and 8.7 to 2.1 cm high (tapering anteriorly). Both hemi-mandibles mark a convex curve anteriorly, terminating in the symphysis.

The dermal ornamentation, visible on the labial side, is almost exclusively composed of pits, as is the case on the skull roof. The mandibular sensory canals running along the surangular and the dentary are deep and well developed (Figs 5A, 5B and see below). This differentiates *A. azerouali* comb. nov. from other metoposaurids.

The dentary broadens anteriorly and forms the mandibular symphysis which is very long (4.4 cm), as in most stereospondyls (e.g., Yates and Warren 2000). It contacts the prearticular postero-lingually and the surangular postero-labially. Its labial surface is slightly ornamented antero-ventrally. It is the only bone bearing large teeth (24 teeth on MNHN.F.ARG 3, between 29 and 72 mm high) and a symphyseal tusk anteriorly (1.2 cm in diameter and 1.0 cm high on MNHN.F.ARG 4), as in all metoposaurids. No alveoli could be observed, but this may be due to the preservation of the specimen.

The three coronoids are typical of metoposaurids: they bear no dentition, contrary to close outgroups such as *Callistomordax* (Schoch 2008). The anterior coronoid is the shortest and the posterior one the longest (3.9 and 11.2 cm long respectively). These coronoids contact the dentary along their dorsal margins. Ventrally, the anterior coronoid contacts the splenial, and the inter- and postero-coronoids contact the postplenial.

The splenials (i.e., splenial *sensu stricto* and postsplenial) are located anteroventrally along the hemi-mandible. They are ornamented with small pits on their labial surface.

The splenial is subrectangular and elongate in lingual view, extending from the middle of the dentary to the beginning of the convex curve of the mandible. It does not contribute the symphysis, contrary to all metoposaurids except *D. ouazzoui* (Dutuit 1976).

The postsplenial is subtriangular and elongate in lingual view, extending from the beginning of the preglenoid region to the middle of the dentary. It is pierced by a small ellipsoid anterior Meckelian fenestra (1.3 cm long). Dutuit (1976, pl. 75) noticed the presence of three splenials on the right hemi-mandible MNHN.F.ARG 3 but only two on the left one MNHN.F.ARG 4. As we did not observe any presplenial on all the available hemi-mandibles, we do not confirm this asymmetry and think *A. azerouali* comb. nov. has only two splenials, as in all temnospondyls (e.g., Jupp and Warren 1986).

The posterior Meckelian fenestra is subtriangular and elongate (Fig. 5D). In contrast, most metoposaurids show a relatively short fenestra. It is formed by the postsplenial dorsally and anteroventrally and the angular ventrally and posteriorly with a weak contribution of the prearticular postero-dorsally (as in all metoposaurids, Jupp and Warren 1986).

The Postglenoid Region (PGR) is relatively short (7.0 cm on MNHN.F.ARG 3) and composed of the articular dorsally, the surangular labially and the articular and angular lingually, but not the prearticular (see description below). As noted by Sulej (2007), the PGR of metoposaurids does not correspond to the typology given by Jupp and Warren (1986), as it bears characters from both "type I" (e.g. prearticular not extending into the PGR) and "type II" (e.g. angular extending into the PGR). In *A. azerouali* comb. nov., the PGR bears a strong ridge formed by the surangular laterally, and a strong postglenoid process. In lingual view, this postglenoid process is slightly higher than the preglenoid process (Fig. 5D).

The prearticular does not extend anteriorly to the anterior border of the adductor fossa, as in all metoposaurids (Jupp and Warren 1986). It contacts the postsplenial anteriorly, the articular posteriorly and the angular ventrally. It bears two dorsal processes on each side of the adductor fossa; a small process on the same level as the preglenoid process (see surangular below) and the postglenoid process posteriorly, contrary to *A. gregorii* which does not present mandibular processes (Spielmann and Lucas 2012). Contrary to *M. krasiejowensis*, the prearticular of *A. azerouali* comb. nov. does not extend posteriorly into the PGR.

The angular, the most ventral bone posteriorly, is elongate and covers a large surface of the hemi-mandible labially. It is subrectangular in lingual view and subtriangular in labial view, starting in the PGR, extending to the middle of the dentary and tapering anteriorly. Its labial surface is very ornamented, bearing numerous pits and small grooves. On its lingual surface, the angular contacts the postsplenial anteriorly, the posterior Meckelian fenestra anterodorsally,

the prearticular dorsally and the articular posterodorsally. On its labial surface, the angular contacts the postsplenial anteriorly, the dentary dorsally and the surangular posteriorly.

The articular is the most posterior bone dorsally. It is mostly visible in lingual view (Fig. 5D) where it is subtriangular and as long as the postglenoid region. It contacts the prearticular anteriorly, the angular ventrally and borders the glenoid fossa dorsally. It projects posteriorly with the retroarticular process.

The surangular is the most dorsal bone posteriorly in labial view. Visible in labial view (Fig. 5B), it is very ornamented, with numerous pits. It bears the preglenoid process dorsally anterior to the glenoid fossa, contrary to *A. gregorii* which does not present mandibular processes (Spielmann and Lucas 2012).

The mandible bears three lateral line canals: the accessory, superior and inferior mandibular canals (Fig. 5B). All canals connect on the posteroventral corner of the surangular.

The accessory mandibular canal is dorsally positioned on the labial surface. It is wide (width of about 1 cm) but relatively short, and barely extending near the postglenoid region. It begins at about a third length of the surangular, marks a convex curve posteroventrally and ends on the retroarticular process with all other mandibular canals.

The superior mandibular canal is the longest, almost extending along the whole length of the labial surface, and narrowing anteriorly (width of 1 cm posteriorly and 0.5 cm anteriorly). It runs along the dentary, reaches the most dorsal margin on the angular, and gently decreases posteriorly on the surangular, untill the posteroventral corner of this bone where it connects the other mandibular canals.

The inferior mandibular canal is ventrally positioned on the labial surface. It is 1 cm wide but relatively short. It begins ventrally at about half length of the angular, extends on the

labial surface, and ends on the posteroventral corner of the surangular where it connects the other mandibular canals.

Postcranial elements

We describe here articulated scapular elements and an isolated radius. The scapular elements, visible on MNHN.F.ARG 9.1-3 (Fig. 6), consist of two sub-complete clavicles and their articulated but incomplete interclavicle, designated as paratypes by Dutuit (1976). As for the cranial bones, these elements are very thick (about 1 cm). The interclavicle is 24.2 cm long and 31.5 cm wide; whereas the left and right clavicles are 26.2 and 23.7 cm long and 14.4 and 15.5 cm wide. These elements are strongly ornamented ventrally: a large region around their ossification centers (i.e. the center of the interclavicle and the posterolateral corner of the clavicles, Hunt 1993) presents polygonal and large alveoli (i.e 'pits'), which turn progressively into deep and elongate grooves radially.

The clavicles are broad and wing-shaped, tapering anteriorly. Their ornamented region bearing alveoli occupy around 20% of the left clavicle MNHN.F.ARG 9.2 and 25% of the right clavicle MNHN.F.ARG 9.3. Their contact zone with the interclavicle is reduced in ventral view, and their medial margins are straight. These clavicles differ from those of the European *Metoposaurus* species which bear a proportionally smaller alveolar ornamented region, an anterior indentation of their medial margin and a longer contact zone with the interclavicle (Colbert and Imbrie 1956; Hunt 1993; Long and Murry 1995; Sulej 2002, 2007). The clavicles of *A. azerouali* comb. nov. also bear ventrally a short and curved canal located in their lateral corners (Fig. 6). This clavicular canal begins on the posterior part of the lateral margin and ends on the anterolateral part of the posterior margin.

The lateral margin of the clavicle is folded vertically and forms a broad dorsal clavicular process. This process is often broken and thus its orientation varies in the studied specimens: it projects medially (e.g. MNHN.F.ARG 9.2, MNHN.F.ARG 8: left clavicle, Dutuit 1976, fig. 76, pl. 42B) or laterally (e.g. MNHN.F.ARG 9.3, MNHN.F.ARG 1: right clavicle fragment, Dutuit 1976, pl. 40B, C).

Ventrally, the interclavicle bears an alveolar ornamented region which is large (around 18% of its total surface), contrary to all *Metoposaurus* species where it is much smaller. The interclavicle of *A. azerouali* comb. nov. also bears two unornamented processes on which the clavicles make contact. It is slightly concave dorsally, gently culminating above its ossification center.

An isolated radius is preserved on MNHN.F.TAL 12 (Fig. 7): it is 9.51 cm in length, the proximal epiphysis is 2.44 cm wide, the distal epiphysis is 1.75 cm wide and the diaphysis is 1.14 cm in diameter. Relatively elongate with flat surfaces, it is similar to the radius of *D. ouazzoui* (Dutuit 1976). Further preparation is needed before a detailed description of this bone can be given.

DISCUSSION

Phylogeny

In order to test the systematic position of the species "*Metoposaurus*" *azerouali* within Metoposauroidea, a phylogenetic analysis was performed. We took into account all currently recognized metoposaurid species; i.e., *Apachesaurus gregorii* (we considered as valid, see above), *Arganasaurus azerouali* comb. nov., *Arganasaurus lyazidi*, *Dutuitosaurus ouazzoui, Koskinonodon bakeri, Koskinonodon maleriensis, Koskinonodon perfectus, Metoposaurus algarvensis, Metoposaurus diagnosticus* and *Metoposaurus krasiejowensis*; and the

metoposauroids *Callistomordax kugleri* and *Almasaurus habazzi* Dutuit, 1972. We also used the basal stereospondyl *Rhineceps nyasaensis* (Haughton, 1927) and the basal temnospondyls *Trimerorachis insignis* Cope, 1878 and *Eryops megacephalus* Cope, 1877 as outgroups.

We built a new matrix of 15 taxa and 63 characters (43 cranial, 9 mandibular, 8 axial skeleton and 3 appendicular skeleton, see Buffa *et al.* 2018, appendix 1, 2) using Mesquite 3.2 (Maddison and Maddison 2017). We consider this analysis preliminary because our matrix is based on a modified and synthetic version of the matrices of McHugh (2012), Milner and Schoch (2013), Schoch (2013), and Marsicano *et al.* (2017): we therefore recoded most character states (characters 1, 3-6, 9-12, 14, 16, 17, 19-22, 26-29, 31-37, 39, 42, 44, 46-48, 52-63) but also defined new ones (characters 2, 7, 8, 13, 15, 18, 23-25, 30, 38, 40, 41, 43, 45, 49-52) based on direct observations (see Buffa *et al.* 2018, appendix 1). Our analysis is the first computer-based phylogeny of the Metoposauridae because the previous works cited above did not consider all the metoposaurid species and the analyses of Hunt (1993) and Sulej (2007) were not based on computerized parsimony.

Our analysis was performed using PAUP* 4 (Swofford 2003) using heuristic searches under the simple stepwise addition sequence and the tree bisection reconnection (TBR) algorithm (reconnection limit = 8). Branches with a maximum length of zero were collapsed. All the character states have the same weight and are considered as non-additive and unordered. We obtained three most parsimonious trees with a length of 143 steps, a Consistency Index (CI) of 0.5385 and a Retention Index (RI) of 0.6118. Both ACCTRAN and DELTRAN options were tested to study the optimization of the character states. All synapomorphies found by PAUP*4 (under both ACCTRAN and DELTRAN options) were studied individually and were considered as unambiguous or not, when both options were congruent (see Buffa *et al.* 2018, appendix 3 for the complete list). The strict consensus tree, mapped on the stratigraphical chart of the middle and Late Triassic, is visible on Figure 8.

The result is that the species *"Metoposaurus" azerouali* forms a robust clade with *Arganasaurus lyazidi*, supporting its attribution within the genus *Arganasaurus* and our new assignment as *Arganasaurus* (*Metoposaurus) azerouali* (Dutuit, 1976) comb. nov. This robust *Arganasaurus* clade (Node G, Fig. 8) is supported by two unambiguous synapomorphies (buldge-like tabular horn and exoccipital process visible in dorsal view) and two ambiguous synapomorphies (cultriform process of uniform width and subtriangular posterior Meckelian fenestra). We previously underlined in the description of *A. azerouali* comb. nov. (see above) that these two taxa also shared a subtriangular squamosal, but since this character could be subjected to individual variation (Spielmann and Lucas 2012), we refrained from using it in our phylogenetic analysis.

Our analysis also shows that the species *M. diagnosticus* from Germany, *M. krasiejowensis* from Poland and *M. algarvensis* from Portugal form a clade (Node L, Fig. 8) supported by three unambiguous synapomorphies (no septomaxilla; prolonged clavicular contact; reduced pits zone in interclavicle ornamentation) and one ambiguous synapomorphy (lacrimal compact). This confirms the hypothesis of Brusatte *et al.* (2015) for whom *Metoposaurus* is a central Laurasian genus. This *Metoposaurus* clade shares synapomorphies with species of *Koskinonodon* (e.g., Nodes J-K, Fig. 8), which yet appear as stem-taxa of *Metoposaurus*. Indeed, none of the *Koskinonodon* species form a clade here, which questions the monophyly of this genus. This could be linked to the fact that a lacrimal entering the orbit was considered as diagnostic by Hunt (1993) to define *Koskinonodon*, although this character is also found in the genus *Metoposaurus* (Sengupta 2002; Sulej 2002, 2007; Brusatte *et al.* 2015).

The species "*Apachesaurus*" *gregorii*, which was considered here as valid to test its position, appears to be sister-taxa to *Koskinonodon perfectus* (they both form a robust clade supported by six unambiguous synapomorphies, see Node I, Fig. 8 and Buffa *et al.* 2018,

appendix 3): this supports the hypothesis of Gee and Parker (2017, 2018a, b) and Gee *et al.* (2017) for whom "*Apachesaurus*" *gregorii* may be a juvenile form of a large metoposaurid, potentially *K. perfectus*.

Our results also suggest that *Dutuitosaurus ouazzoui* is the most basal metoposaurid, as considered by Hunt (1993) but *contra* Schoch and Milner (2000). At least, the robust family Metoposauridae (Node E, Fig. 8; see Systematic Palaeontology above for diagnosis and definition) is comprised, with *Almasaurus habazzi* and *Callistomordax kugleri*, in the other robust and more inclusive clade Metoposauroidea which is supported by five unambiguous synapomorphies and two ambiguous synapomorphies (see Buffa *et al.* 2018, appendix 3).

Stratigraphic distribution

Before dealing with the evolution of the metoposaurids, a state-of-the-art of their stratigraphic distribution has been compiled according to the literature and is visible on Figure 9. It encompasses several stages. Note that the stratigraphic ages of some taxa are not precise and the duration of some (sub)stages is debated (see Fig. 9). The temporal limits of the Norian indeed vary according to the authors: either 220-208.5 Ma ("short Norian" hypothesis of Muttoni *et al.* 2004; Lucas 2018a; Lucas and Tanner 2018) or 227-208.5 Ma ("long Norian" hypothesis according to Ogg *et al.* 2014). To minimize the number of working hypotheses in our discussion below, we took into account the longest duration of the Norian (i.e., 227-208.5 Ma).

The metoposauroid *Callistomordax* comes from the Erfurt Formation in Germany (Schoch 2008) dated between 239.5 Ma and 237.5 Ma (Longobardian, late Ladinian, Fig. 9) according to the German Stratigraphic Commission (2016). *M. diagnosticus* is known in the Germanic Keuper (Milner and Schoch 2004) with its first occurrence in the Schilfsandstein

(Stuttgart Formation, beginning at 231.5 Ma, late Julian, "middle" Carnian, German Stratigraphic Commission 2016), and its last occurrence in the Lehrbergschichten (lower Weser Formation, last unit of the Carnian, ending at ca. 227 Ma, Cohen *et al.* 2018).

The Polish Krasiejów bonebed has long been considered late Carnian based on its vertebrate assemblage and on a correlation with the German Lehrbergschichten (Dzik 2001, 2003; Dzik and Sulej 2007; Sulej 2002, 2007). However, recent litho-, bio-, climato- and chemostratigraphic correlations attribute this bonebed to the Norian, i.e. coeval with the lowest strata of the "Middle Grey Sandstones" of the German Arnstadt Formation (= Stubensandstein, K5 Unit of the Keuper, Fig. 9, see Milner and Schoch 2004; Szulc 2005, Szulc *et al.* 2015). In Germany, *M. krasiejowensis* is found in the Kielsandstein (upper Weser Formation, Milner and Schoch 2004) which is the first unit of the Norian. Note that Milner and Schoch (2004) also attributed the German specimen BMNH 37938 from Aixheim to *M. krasiejowensis*, therefore coming to the Middle Stubensandstein, of similar age to the Polish specimens, but Lucas *et al.* (2007b) and Lucas (2015) argued against this stratigraphic attribution. The stratigraphic distribution of *M. krasiejowensis* thus extends from the Carnian-Norian boundary (ca. 227 Ma, Cohen *et al.* 2018) to the lower K5 unit of the Keuper (ca. 218.5-209.5 Ma, German Stratigraphic Commission 2016).

Metoposaurus and the phytosaur *Parasuchus* have long been used to define the Otischalkian and Adamanian Carnian Land Vertebrate Faunachrons (LVF) (e.g. Lucas 1998, 2010, 2018b; Lucas *et al.* 2007a, 2012 Lucas and Tanner 2014). *Metoposaurus* is thus not thought to extend into the Revuletian, the first and longest LVF of the Norian. However, as just shown, *Metoposaurus* does extend into the Norian both in Germany and Poland (Figs 8, 9), and *Parasuchus* is also present in the Norian Krasiejów bonebed (Dzik and Sulej, 2007; Lucas, 2018b). This is also the case under the "short Norian" hypothesis, in which the Krasiejów bonebed is situated at the base of the Norian stage (Szulc *et al.* 2015).

Lucas (2018b) partly defined the Otischalkian substage based on the highest occurrence of the almasaurids. However, as *Latiscopus disjunctus* Wilson, 1948 is a *nomen dubium* (Bolt and Chatterjee 2000) and the "lettenkeuper almasaurid" of Schoch and Milner (2000) belongs to *Callistomordax* (Schoch, 2008), the family Almasauridae is only known from a single locality and horizon in Morocco and cannot be used as index taxa. The LVFs of Lucas (2018b) are thus questionable (and not used here) because *Metoposaurus* and *Almasaurus* cannot be considered as indicators of the Carnian. Further studies will test whether the Adamanian LVF extends into the Norian (as proposed by Imris *et al.* 2010, Martz *et al.* 2013 and Ogg *et al.* 2014) or not. Pending these studies, the Otischalkian to Adamanian age of the Indian, North American, Moroccan and Portugese metoposaurids given by Lucas (2018b) are not taken into account in our discussion below.

The Portuguese *M. algarvensis* is from the Penina bonebed of the 'AB2' Unit of the Algarve Basin. This unit is considered as latest Carnian-early Norian in age based on the co-occurrence of *M. algarvensis* with a phytosaur indet. (Steyer *et al.* 2011; Mateus *et al.* 2014; Brusatte *et al.* 2015) and on biostratigraphic correlations (conchostracans, bivalves, macro- and micro-flora) with the Spanish Cofrentes Formation (Arche and López-Gómez 2014). The Cofrentes Formation lays above strata correlated with the German Schilfsandstein, ending at 229.5 Ma (Tuvalian, late Carnian, Arche and López-Gómez 2014; German Stratigraphic Commission 2016). This will be considered a minimum age for the base of the Portuguese 'AB2' Unit.

The Indian *K. maleriensis* comes from the Lower Maleri (Pranhita-Godavari Basin) and the Tiki formations (Rewa Basin) (Sengupta 2002, 2003). These formations are considered coeval based on faunal and floral similarities (Mukherjee *et al.* 2012, Ray *et al.* 2016). Both are correlated to the lower Ischigualastian fauna of the Ischigualasto Formation on the basis of faunal resemblance, and are part of the *Hyperodapedon* Assemblage Zone, commonly used to

correlate Gondwanan formations (Langer 2005; Bandyopadhay and Sengupta 2006; Ray *et al.* 2016). The Ischigualasto Formation is bracketed by two volcanic layers, respectively dated 231.4 ± 0.3 Ma and 225.9 ± 0.9 Ma (late Julian-Tuvalian, late Carnian, Martinez *et al.* 2011; Kent *et al.* 2014; Langer *et al.* 2018). In the absence of precise dating for the Indian formations, we consider *K. maleriensis* to be constrained between these brackets (Fig. 9).

The oldest North American metoposaurids (i.e., first occurrence of *K. perfectus* and unique occurrence of *K. bakeri*) come from the Santa Rosa Sandstone and the coeval Camp Springs Member of the Dockum Group and Evangeline Member of the Wolfville Formation (Long and Murry 1995; Schoch and Milner 2000; Martz *et al.* 2013; Sues and Olsen 2015). The Santa Rosa Sandstone is overlain by the Tecovas Member (first occurrence of *A. gregorii*, *K. perfectus*, Long and Murry 1995; Schoch and Milner 2000), which has been correlated with the Blue Mesa and Sonlesa members of the Chinle Formation based on numerous faunal similarities (Martz *et al.* 2013). As a result, the oldest metoposaurid-bearing strata are rough equivalents of the underlying Shinarump and Mesa Renondo members, the oldest of the Chinle Formation, dated between 227 and 225 Ma (Lacian, early Norian, Ramezani *et al.* 2014).

The highest occurrences of metoposaurids in North America come from the upper part of the Petrified Forest Member of the Chinle Formation (*A. gregorii*, *K. perfectus*) and the upper Redonda Formation of the Dockum Group (*A. gregorii*, Hunt 1993; Long and Murry 1995; Schoch and Milner 2000; Spielmann and Lucas 2012). The Petrified member specimens come from under the Black Forest Bed, dated just under 210 Ma, in the latest Norian (Ramezani *et al.* 2014; Gee and Parker 2018a). We consider this age as minimum for the Redonda Formation, which is stratigraphically higher than the Petrified Forest Member (Fig. 9, Martz *et al.* 2013).

The Moroccan metoposaurids all come from the Irohalène Member ("T5" unit *sensu* Dutuit, 1976, Timezgadiouine Formation) of the Argana Basin. This unit has traditionally been considered of Carnian age based on its faunal assemblage (Khaldoune *et al.* 2017). The

underlying Aglégal Member ("T4" unit *sensu* Dutuit 1976) has been dated as Middle Triassic (Anisian-Ladianian) based on charophytes, ostracods and vertebrate remains (Medina *et al.* 2001; Jalil *et al.* 2009, Khaldoune *et al.* 2017). Microfloral remains have suggested a late Carnian-earliest Norian age for the overlying Tadrarat Ouadou Member ("T6" unit *sensu* Dutuit 1976, Bigoudine Formation; Tourani *et al.* 2000; Khaldoune *et al.* 2017). As there is no apparent discontinuity between the T4 and T5 units, the T5 unit may comprise the early Carnian and at least part of the late Carnian. However we cannot attribute more precise ages for these "lower" and "upper" horizons of Dutuit (1976) (Fig. 9).

Evolution of the Metoposauridae

According to the phylogeny obtained and the stratigraphic and geographic distributions of the considered taxa (Figs 8, 9), we can propose evolutionary scenarios for the metoposaurid origin, diversification and extinction:

As *Callistomordax kugleri* from the Longobardian (upper Ladinian) of Germany (Schoch 2008) is the oldest known metoposauroid (Fig. 8), the ages of divergence of both the clade (*Callistomordax* + Metoposauridae) and the Metoposauridae may be Longobardian or older. Since *Almasaurus* (sister-taxon to the clade *Callsitomordax* + Metoposauridae) and *Dutuitosaurus* (basal metoposaurid) are Moroccan, these divergences may have occurred in central Pangea, around southern Laurasia or northern Gondwana.

The German *M. diagnosticus* and the Indian *K. maleriensis* are the oldest metoposaurids whose first occurrences are well constrained (ca. 231.5-231 Ma, late Julian-early Tuvalian, "middle" Carnian, Fig. 8). Their almost simultaneous appearance in Laurasian and Gondwanan formations suggest a rapid diversification of the Metoposauridae. Their first occurrence is coeval with the Carnian Pluvial Episode (CPE; Simms and Ruffell 1989; Ruffell *et al.* 2016), a

global climate change in the late Julian ("middle" Carnian, 1.2 Ma long and ending at ca. 231 Ma according to Dal Corso *et al.* 2018) during which the climate turned from arid to humid and then to arid again (Figs 8, 9). As metoposaurids occupied freshwater environments (Hunt 1993; Schoch and Milner 2000; Brusatte *et al.* 2015), they may have benefited from an increasing number of large freshwater areas during that time. As argued by Fortuny *et al.* (2017), the large-sized metoposaurid species indeed thrived in large freshwater bodies. The CPE could therefore have favored the metoposaurid diversification, as it was also proposed for the dinosaur radiation (Bernardi *et al.* 2018), but further studies will test this hypothesis. In particular, a more precise dating of the Moroccan metoposaurid bonebeds is needed before a strong correlation between the CPE and the metoposaurid diversification can be made.

As the earliest diverging taxa (*D. ouazzoui*, *A. lyazidi* and *A. azerouali*) are Moroccan, this diversification of the Metoposauridae may have occurred in northern Gondwana first, then in western Laurasia (neighbor province near the palaeoequator in the Late Triassic, Brusatte *et al.*, fig. 13), then in eastern Gondwana (India, *K. maleriensis*) and eastern Laurasia (*Metoposaurus*).

To explain the occurrence of *K. maleriensis* in higher palaeolatitudes in the late Carnian of India, Sengupta (2002, 2003) proposed that metoposaurids could have used circum-tethyan shoreline connections. This possible circum-tethyan dispersion is also supported by the fact that all the metoposaurid localities were in a summerwet climatic biozone according to the model of Selwood and Valdes (2006, see also Brusatte *et al.* 2015). However, the current metoposaurid fossil record is still too sparse to support a robust scenario explaining their dispersion.

In the Norian (following the commonly accepted "long Norian" hypothesis, Muttoni *et al.* 2004; Ogg *et al.* 2014; Cohen *et al.* 2018), metoposaurids appear to be mostly located in Laurasia, with only *K. maleriensis* potentially extending in Gondwana (India) during the earliest Norian (Figs 8, 9). Fortuny *et al.* (2017) proposed that the aridification of the climate during

the Norian may have led to the decline of metoposaurids. These authors argued that the group underwent a trend in size diminution during the Norian, as diminutive taxa such as *A. gregorii* would have been better suited to arid climates, which is why they are more represented in these horizons. This trend in size diminution has been refuted by Gee and Paker (2017, 2018a) on the basis of *A. gregorii* being a juvenile metoposaurid, and evidence shows that the metoposaurids could withstand some variety of climates (Konietzko-meier and Klein 2013). However, metoposaurids are indeed rarer in the higher Norian horizons. In addition, it has been proposed that in nonmarine environments, the unspecialized metoposaurids may have faced difficulties competing with more specialized taxa, especially suction feeders such as the piscivorous phytosaurs (Schoch and Milner 2000) and the brachyopoids and plagiosaurids (whom vaulted palate is specialized in suction feeding, see Warren *et al.* 2000; Sengupta 2003). Further studies are needed to test this hypothesis. Following their decline during the Norian, metoposaurids are only represented by isolated material non-diagnostic beyond the family level in the Rhaetian of North America (Spielmann *et al.* 2007).

CONCLUSION

The systematic revision and detailed redescription of "*Metoposaurus*" *azerouali* Dutuit, 1976 from the Late Triassic of Morocco have highlighted its close relationship with *Arganasaurus lyazidi* and led to the new combination *Arganasaurus* (*Metoposaurus*) *azerouali* (Dutuit, 1976) comb. nov., proposed here. Its comparison with other metoposaurids led to the first phylogeny of the Metoposauridae, which confirms that the genus *Metoposaurus* is composed of central Laurasian species and supports the hypothesis that "*Apachesaurus*" *gregorii* may be a juvenile form of *Koskinonodon perfectus* known in the Norian of North

America. The current fossil record of the Metoposauroidea together with the phylogeny obtained suggest that the group diverged at least during the Longobardian (late Ladinian), and diversified around the late Julian ("middle" Carnian). This diversification could be linked to the Carnian Pluvial Episode (CPE), a global climate change from arid to humid conditions coeval with the first strongly constrained occurrences of metoposaurids. Metoposaurids may have diversified first in northern Gondwana and then in western Laurasia, southern Gondwana and central Laurasia, in tropical humid biomes. Their decline may be linked to the aridification of the climate in the Norian and competition with other more specialized taxa, leading to their extinction in the Rhaetian in North America.

Acknowledgements. We thank V. Barriel (MNHN) for her phylogenetic help to V.B., P. Loubry (CNRS Paris) for the photos of the studied specimens, D. Germain (MNHN), G. Clément (MNHN) and S. Crasquin (CNRS) for their authorization to study the material. We thank C. Marsicano and two anonymous reviewers for their constructive reviews, and S. Thomas and K. Angielczyk for their editorial works.

DATA ARCHIVING STATEMENT

Data for this study are available in the Dryad Digital Repository: https://datadryad.org/review?doi=doi:10.5061/dryad.d6s5h2d **[please note that the data for this paper are not yet published and this temporary link should not be shared without the express permission of the author]**

File 1. Character-taxon matrix.

SUPPORTING INFORMATION

Additional Supporting Information can be found in the online version of this article

Appendix S1. Description of characters used in phylogenetic analysis.

Appendix S2. Character states for each taxon.

Appendix S3. List of nodes returned by phylogenetic analysis with ambiguous and unambiguous synapomorphies.

FIG. S1. Character 2: Shape of orbits. All character states are represented.

FIG. S2. Character 7: Lacrimal-nasal suture. All character states are represented. Lacrimal in light gray, nasal in dark gray.

FIG. S3. Character 8: Lacrimal shape. All character states are represented. Lacrimal in light gray.

FIG. S4. Character 13: Postfrontal contribution to orbital margin. All character states are represented. Postfrontal in light gray.

FIG. S5. Character 18: Postorbital sulcus-posterior skull margin contact. All character states are represented. Supraorbital canal in light gray, infraorbital and postorbital canal in dark gray.

FIG. S6. Character 23: Transverse pterygoid flange. All character states are represented.

FIG. S7. Character 24: Palatine ramus medial margin. All character states are represented.

FIG. S8. Character 25: Parasphenoid ornamentation. All character states are represented.

FIG. S9. Character 30: Orbits in interpterygoid fenestrae. All character states are represented.

FIG. S10. Character 38: Paraquadrate accessory foramen. All character states are represented.

FIG. S11. Character 40: Foramen magnum shape. All character states are represented.

FIG. S12. Character 41: Foramen magnum proportions. All character states are represented.

FIG. S13. Character 45: Anterior coronoid tooth row. All character states are represented.

FIG. S14. Character 49: Splenial contribution to symphysis. All character states are represented. Splenial in light gray.

FIG. S15. Character 50: Posterior Meckelian fenestra shape. All character states are represented.

FIG. S16. Character 51: Mandibular anterior ventral margin. All character states are represented.

FIG. S17. Character 52: Mandibular tapering in height anteriorly. All character states are represented.

REFERENCES

ARCHE, A. and LÓPEZ-GÓMEZ, J. 2014. The Carnian Pluvial Event in Western Europe: new data from Iberia and correlation with the Western Neotethys and Eastern North America–NW Africa regions. *Earth-Science Reviews*, **128**, 196–231.

BANDYOPADHYAY, S. and SENGUPTA, D. P. 2006. Vertebrate faunal turnover during the Triassic-Jurassic transition: an Indian scenario. *New Mexico Museum of Natural History and Science Bulletin*, **37**, 77–85.

BERNARDI, M., GIANOLLA, P., PETTI, F. M., MIETTO, P. and BENTON, M. J. 2018. Dinosaur diversification linked with the Carnian Pluvial Episode. *Nature Communications*, **9**, 1–10.

BOLT, J. R. and CHATTERJEE, S. 2000. A new temnospondyl amphibian from the Late Triassic of Texas. *Journal of Paleontology*, **74** (4), 670–683.

BOY, J. A. 1974. Die Larven der rhachitomen Amphibien (Amphibia: Temnospondyli; Karbon-Trias). *Paläontologische Zeitschrift*, **48**, 236–268.

BRUSATTE, S. L., BUTLER, R. J., MATHEUS, O. and STEYER, J.-S. 2015. A new species of *Metoposaurus* from the Late Triassic of Portugal and comments on the systematics and biogeography of metoposaurid temnospondyls. *Journal of Vertebrate Paleontology*, **35** (3), 1–23.

BUFFA, V., JALIL, N. –E, STEYER, J. –S. 2018. Data from : Redescription of *Arganasaurus* (*Metoposaurus) azerouali* (Dutuit) comb. nov. from the Late Triassic of the Argana Basin (Morocco), and the First Phylogenetic Analysis of the Metoposauridae (Amphibia, Temnospondyli). *Dryad Digital Repository*. https://doi.org/10.5061/dryad.d6s5h2d

CASE, E. C. 1922. New reptiles and stegocephalians from the Upper Triassic of western Texas. *Carnegie Institution of Washington*, **321**, 7–84.

— 1931. Description of a new species of *Buettneria* with a discussion of the brain case. *Contributions from the Museum of Paleontology, University of Michigan*, **3**, 187–206.

CHOWDHURY, T. R. 1965. A new metoposaurid amphibian from the upper Triassic Maleri Formation of Central India. *Philosophical Transaction of the Royal Society of London, Series B*, **250**, 1–52.

COHEN, K. M., FINNEY, S. C., GIBBARD, P. L. and FAN, J.-X. 2018 (2013; updated). The ICS International Chronostratigraphic Chart. Episodes **36**, 199–204.

COLBERT, E. H. and IMBRIE, J. 1956. Triassic metoposaurid amphibians. *Bulletin of the American Museum of Natural History*, **110**, 402–452.

COPE, E. D. 1877. Description of extinct Vertebrate from the Permian and Triassic formations of the United States. *Proceedings of the American Philosophical Society*, **17**, 182–193.

— 1878. Description of extinct Batrachia and Reptilia from the Permian Formation of Texas. *Proceedings of the American Philosophical Society*, **17**, 505–530.

CORROY, G. 1928. Les vertébrés du Trias de Lorraine et le Trias Lorrain. *Annales de Paléontologie*, **17**, 83–136.

CUNY, G. and RAMBOER, G. 1991. Nouvelles données sur la faune et l'âge de Saint Nicholas de Port. *Revue de Paléontologie*, **10**, 69–78.

DAL CORSO, J., BENTON, M. J., BERNARDI, M., FRANZ, M., GIANOLLA, P., HOHN, S., KUSTATSCHER, E., MERICO, A., ROGHI, G., RUFFELL, A., Ogg, J. G, PRETO, N. SCHMIDT, A. R., SEYFULLAH, L. J., SIMMS, M. J., SHI, Z. and ZHANG, Y. 2018. First workshop on the Carnian Pluvial Episode (Late Triassic): a report. *Albertiana*, **44**, 49–57.

DAMIANI, R. J. and YATES, A. M. 2003. The Triassic amphibian *Thoosuchus yakovlevi* and the relationships of the Trematosauroidea. *Records of the Australian Museum*, **55**, 331–342.

DUTUIT, J. M. 1972. Un nouveau genre de stégocéphale du Trias supérieur marocain : *Almasaurus habbazi*. *Bulletin du Muséum National d'Histoire Naturelle, Série C, Sciences de la Terre*, **72**, 73–81.

— 1976. Introduction à l'étude paléontologique du Trias continental marocain : Description des premiers Stégocéphales recueillis dans le couloir d'Argana (Atlas occidental).

Mémoires du Muséum National d'Histoire Naturelle, Série C, Sciences de la Terre, **36**, 253 pp.

— 1978. Description de quelques fragments osseux provenant de la région de Folakara (Trias supérieur malgache). *Bulletin du Muséum National d'Histoire Naturelle, Série C, Sciences de la Terre,* **69**, 79–89.

DZIK, J. 2001. A new *Paleorhinus* fauna in the early Late Triassic of Poland. *Journal of Vertebrate Paleontology*, **21** (3), 625–627.

— 2003. A beaked herbivorous archosaur with dinosaur affinities from the early Late Triassic of Poland. *Journal of Vertebrate Paleontology*, **23** (3), 556–574.

— and SULEJ, T. 2007. A review of the early Late Triassic Krasiejów biota from Silesia, Poland. *Acta Paleontologia Polonica*, **64**, 3–27.

FORTUNY, J., MARCÉ-NOGUÉ, J. and KONIETZKO-MEIER, D. 2017. Feeding biomechanics of Late Triassic metoposaurids (Amphibia: Temnospondyli): a 3D finite element analysis approach. *Journal of Anatomy*, **230**, 752–765.

GEE, B. M. and PARKER, W. G. 2017. A juvenile *Koskinonodon perfectus* (Temnospondyli, Metoposauridae) from the Upper Triassic of Arizona and its implications for the taxonomy of North American metoposaurids. *Journal of Paleontology*, **18**, 1–13.

— and PARKER, W. G. 2018a. A large-bodied metoposaurid from the Revueltian (late Norian) of Petrified Forest National Park (Arizona, USA). *Neues Jahrbuch für Geologie und Paläontologie – Abhandlungen*, **287**, 61–73.

— and PARKER, W. G. 2018b. Morphological and histological description of small metoposaurids from Petrified Forest National Park, AZ, USA and the taxonomy of *Apachesaurus*. *Historical Biology*, DOI: 10.1080/08912963.2018.1480616

—, PARKER, W. G. and MARSH, A. D. 2017. Microanatomy and paleohistology of the intercentra of North American metoposaurids from the Upper Triassic of Petrified Forest National Park (Arizona, USA) with implications for the taxonomy and ontogeny of the group. *PeerJ*, **5**, e3183.

GERMAN STRATIGRAPHIC COMMISSION. 2016. (ed.; editing, coordination and layout: Menning, M. and Hendrich, A.): Stratigraphic Table of Germany 2016. Potsdam (German Research Centre for Geosciences).

GREGORY, J. T. 1980. The otic notch of metoposaurid labyrinthodonts. *In:* Aspects of Vertebrate History: Essays in Honor of Edwin Harris Colbert. Jacobs, L.L., ed. *Museum of Northern Arizona*, 125–136.

HAUGHTON, S. H. 1927. On Karroo vertebrates from Nyasaland. *Transactions of the Geological Society of South Africa*, **29**, 69–83.

HUNT, A. P. 1993. Revision of the Metoposauridae (Amphibia: Temnospondyli) and description of a new genus from Western North America. *In*: Aspects of Mesozoic Geology and Paleontology of the Colorado Plateau. Morales, M., ed. *Museum of Northern Arizona Bulletin*, **59**, 67–97.

IRMIS, R. B., MARTZ, J. W., PARKER, W. G. and NESBITT, S. J. 2010. Re-evaluating the correlation between Late Triassic terrestrial vertebrate biostratigraphy and the GSSP-defined marine stages. *Albertiana*, **38**, 40–52.

JALIL, N. -E., JANVIER, P. and STEYER, J. -S. (2009). A new cyclotosaurid (Amphibia, Temnospondyli) from the Triassic of Argana Basin (High Atlas Mountains, Morocco); biostratigraphic implications. *In First International Congress on North African Vertebrate Palaeontology, Abstract Volume*, 36–37.

JUPP, R. and WARREN, A. A. 1986. The mandibles of the Triassic temnospondyl amphibians. *Alcheringa*, **10**, 99–124.

KENT, D. V., MALNIS, P. S., COLOMBI, C. E., ALCOBER, O. A. and MARTINEZ, R. N. 2014. Age constraints on the dispersal of dinosaurs in the Late Triassic from magnetochronology of the Los Colorados Formation (Argentina). *Proceedings of the National Academy of Sciences*, **111** (22), 7956–63.

KHALDOUNE, F., JALIL, N.-E., GERMAIN, D. and STEYER, J.-S. 2017. Les vertébrés du Permien et du Trias du Maroc (Bassin d'Argana, Haut Atlas Occidental) : une fenêtre ouverte sur l'évolution autour de la grande crise fini-paléontologique, 103-166. *In: Bulletin de la Société Géologique de France*, n.s. **180**, 624 pp.

KOKEN, E. 1913. Beiträge zur Kenntnis der Schichten von Heiligkreuz (Abteital, Südtirol). *Abhandlungen der Kaiserlich-Königlichen Geologischen Reichsanstalt*, **16** (4), 1–43.

KONIETZKO-MEIER, D. and KLEIN, N. 2013. Unique growth pattern of *Metoposaurus diagnosticus krasiejowensis* (Amphibia, Temnospondyli) from the Upper Triassic of Krasiejów, Poland. *Palaeogeography, Palaeoclimatology, Palaeoecology*, **370**, 145–157.

KUHN, O. 1932. Labyrinthodonten und Parasuchier aus dem mittleren Keuper von Ebrach in Oberfranken. *Neues Jahrbuch für Mineralogie, Geologie und Paläontologie. Abteilung B*, **69**, 94–144.

LANGER, M. C. 2005. Studies on continental Late Triassic tetrapod biochronology. II. The Ischigualastian and a Carnian global correlation. *Journal of South American Earth Sciences*, **19** (2), 219–239.

—, RAMEZANI, J. and DA ROSA, Á. A. 2018. U-Pb age constraints on dinosaur rise from south Brazil. *Gondwana Research*, **57**, 133–140.

LEHMAN, J.-P. 1971. Nouveaux vertébrés fossils du Trias de la série de Zarzaïtine. *Annales de Paléontologie (Vertébrés)*, **57**, 71–113.

LONG, R. A. and MURRY, P. A. 1995. Late Triassic (Carnian and Norian) tetrapods from the southwestern United States. *Bulletin of the New Mexico Museum of Natural History and Science*, **4**, 254 pp.

LUCAS, S. G. 1998. Global Triassic tetrapod biostratigraphy and biochronology. *Palaeogeography, Palaeoclimatology, Palaeoecology*, **143** (4), 347–384.

— 2010. The Triassic timescale based on nonmarine tetrapod biostratigraphy and biochronology. *Geological Society, London, Special Publications*, **334** (1), 447–500.

— 2015. Age and correlation of Late Triassic tetrapods from southern Poland. *Annales Societatis Geologorum Poloniae*, **85** (4), 627–635.

— 2018a. The Late Triassic Timescale. *In: The Late Triassic World*. Springer, Cham, 1–25.

— 2018b. Late Triassic terrestrial tetrapods: Biostratigraphy, biochronology and biotic events. *In: The Late Triassic World*. Springer, Cham, 351–405.

—, HUNT, A. P., HECKERT, A. B. and SPIELMANN, J. A. 2007a. Global Triassic tetrapod biostratigraphy and biochronology: 2007 status. *New Mexico Museum of Natural History and Science Bulletin*, **41**, 229–240.

—, RINEHEART, L. F., HECKERT, A. B., HUNT, A. P. and SPIELMANN, J. A. 2016. Rotten Hill: A Late Triassic Bonebed in the Texas Panhandle, USA. *New Mexico Museum of Natural History and Science Bulletin*, **72**, 1–97.

—, SPIELMANN, J. A. and HUNT, A. P. 2007b. Biochronological significance of Late Triassic tetrapods from Krasiejów. In: Lucas, S. G. and Spielmann, J. A. (eds), *The Global Triassic. New Mexico Museum of Natural History and Science Bulletin*, **41**, 248–258.

— and TANNER, L. H. 2014. Triassic Timescale Based on Tetrapod Biostratigraphy and Biochronology. *In: STRATI 2013*. Springer, Cham, 1013–1016.

— and TANNER. 2018. Record of the Carnian wet episode in strata of the Chinle Group, western USA. *Journal of the Geological Society*, jgs2017–134.

—, TANNER, L. H., KOZUR, H. W., WEEMS, R. E. and HECKERT, A. B. 2012. The Late Triassic timescale: age and correlation of the Carnian–Norian boundary. *Earth-Science Reviews*, **114** (1-2), 1–18.

LYDEKKER, R. 1890. *Catalogue of the Fossil Reptilia and Amphibia in the British Museum of Natural History. Part IV*. British Museum of Natural History, London, 295 pp.

MADDISON, W. P. and MADDISON, D. R. 2017. Mesquite: a modular system for evolutionary analysis. Version 3.2.

MARSICANO, C. A., LATIMER, E., RUBIDGE, B. and SMITH, R. M. H. 2017. The Rhinesuchidae and early history of the Stereospondyli (Amphibia: Temnospondyli) at the end of the Paleozoic. *Zoological Journal of the Linnean Society*, **20**, 1–28.

MARTINEZ, R. N., SERENO, P. C., ALCOBER, O. A., COLOMBI, C. E., RENNE, P. R., MONTAÑEZ, I. P. and CURRIE, B. S. 2011. A basal dinosaur from the dawn of the dinosaur era in southwestern Pangaea. *Science*, **331** (6014), 206–210.

MARTZ, J. W., MUELLER, B., NESBITT, S. J., STOCKER, M. R., PARKER, W. G., ATANASSOV, M., FRASER, N., WEINBAUM, J. and LEHANE, J. R. 2013. A

taxonomic and biostratigraphic re-evaluation of the Post Quarry vertebrate assemblage from the Cooper Canyon Formation (Dockum Group, Upper Triassic) of southern Garza County, western Texas. *Earth and Environmental Science Transactions of the Royal Society of Edinburgh*, **103** (3–4), 339–364.

MATEUS, O., BUTLER, R. J., BRUSATTE, S. L., WHITESIDE, J. H. and STEYER, J. -S. 2014. The first phytosaur (Diapsida, Archosauriformes) from the Late Triassic of the Iberian Peninsula. *Journal of Vertebrate Paleontology*, **34** (4), 970–975.

MEDINA, F., VACHARD, D., COLIN, J. P., OUARHACHE, D. and AHMAMOU, M. 2001. Charophytes et ostracodes du niveau carbonaté de Taourirt Imzilen (Membre d'Aglegal, Trias d'Argana); implications stratigraphiques. *Bulletin de l'Institut des Sciences*, **23**, 21–26.

MCHUGH, J. B. 2012. Temnospondyl ontogeny and phylogeny, a window into terrestrial ecosystems during the Permian-Triassic extinction. PhD thesis, University of Iowa, 198 pp.

MEYER, E. 1842. Labyrinthodonten—Genera. *Neues Jahrbuch für Mineralogie, Geographie, Geologie, Paläeontologie*, **1842**, 301–304.

MILNER, A. R. and SCHOCH, R. R. 2004. The latest metoposaurid amphibians from Europe. *Neues Jahrbuch fur Geologie und Palaontologie*, **232** (2-3), 231–252.

— 2013. *Trimerorhachis* (Amphibia: Temnospondyli) from the lower Permian of Texas and New Mexico: Cranial osteology, taxonomy and biostratigraphy. *Neues Jahrbuch für Geologie und Paläontologie*, **270**, 91–128.

MOODIE, R. L. 1908. The lateral line system in extinct Amphibia. *Journal of Morphology*, **19**, 511–541.

MUKHERJEE, D., RAY, S., CHANDRA, S., PAL, S. and BANDYOPADHYAY, S. 2012. Upper Gondwana succession of the Rewa basin, India: understanding the interrelationship of lithologic and stratigraphic variables. *Journal of the Geological Society of India*, **79** (6), 563–575.

MUTTONI, G., KENT, D. V., OLSEN, P. E., STEFANO, P. D., LOWRIE, W., BERNASCONI, S. M. and HERNÁNDEZ, F. M. 2004. Tethyan magnetostratigraphy from Pizzo Mondello (Sicily) and correlation to the Late Triassic Newark astrochronological polarity time scale. *Geological Society of America Bulletin*, **116** (9-10), 1043–1058.

OGG, J. G., HUANG, C. and HINNOV, L. 2014. Triassic timescale status: a brief overview. *Albertiana*, **41**, 3–30.

RAMEZANI, J., FASTOVSKY, D. E. and BOWRING, S. A. 2014. Revised chronostratigraphy of the lower Chinle Formation strata in Arizona and New Mexico (USA): high-precision U-Pb geochronological constraints on the Late Triassic evolution of dinosaurs. *American Journal of Science*, **314** (6), 981–1008.

RAY, S., SHAFI BHAT, M., MUKHERJEE, D. and DATTA, P.M. 2016. Vertebrate fauna from the Late Triassic Tiki Formation of India: new finds and their biostratigraphic implications. *The Palaeobotanist*, **65**, 47–59.

RUFFELL, A., SIMMS, M. J. and WIGNALL, P. B. 2016. The Carnian Humid Episode of the late Triassic: a review. *Geological Magazine*, **153** (2), 271–284.

RUTA, M., PISANI, D., LLOYD, G. T. and BENTON, M. J. 2007. A supertree of Temnospondyli: cladogenetic patterns in the most species-rich group of early tetrapods. *Proceedings of the Royal Society of London, Series B*, **274**, 3087–3095.

SCHOCH, R. R. 2008. A new stereospondyl from the Middle Triassic of Germany, and the origin of the Metoposauridae. *Zoological Journal of the Linnean Society*, **152**, 79–113.

— 2011. A trematosaurid temnospondyl from the Middle Triassic of Jordan. *Fossil Record*, **14**, 119–127.

— 2013. The evolution of major temnospondyl clades: an inclusive phylogenetic analysis. *Journal of Systematic Palaeontology*, **11**, 673–705.

— and MILNER, A. R. 2000. *Handbuch der Paläoherpetologie 3B. Stereospondyli: Stem-Stereospondyli, Rhinesuchidae, Rhytidostea, Trematosauridea, Capitosauridea.* Munich: Verlag Dr Friedrich Pfeil, 203 pp.

SELLWOOD, B. W. and VALDES, P. J. 2006. Mesozoic climates: general circulation models and the rock record. *Sedimentary Geology*, **190**, 269–87.

SENGUPTA, D. P. 2002. Indian Metoposaurid Amphibians revised. *Paleontological Research*, **6**, 41–65.

— 2003. Triassic temnospondyls of the Pranhita-Godavari basin, India. *Journal of Asian Earth Sciences*, **21**, 655–662.

SIMMS, M. J. and RUFFELL, A. H. 1989. Synchroneity of climatic change and extinctions in the Late Triassic. *Geology*, **17**, 265–268.

SPIELMANN, J. A. and LUCAS, S. G. 2012. Tetrapod Fauna of the Upper Triassic Redonda Formation, East-Central New Mexico: The Characteristic Assemblage of the Apachean Land-vertebrate Faunachron. *New Mexico Museum of Natural History & Science Bulletin*, **55**, 1–119.

—, LUCAS, S. G. and HECKERT, A. B. 2007. Tetrapod fauna of the Upper Triassic (Revueltian) Owl Rock Formation, Chinle Group, Arizona. *New Mexico Museum of Natural History and Science Bulletin*, **41**, 371–383.

STEYER, J. S. 2000. Ontogeny and phylogeny in temnospondyls: a new method of analysis. *Zoological Journal of the Linnean Society*, **130**, 449–467.

— 2002. The first articulated trematosaur 'amphibian' from the Lower Triassic of Madagascar: implications for the phylogeny of the group. *Palaeontology,* **45**, 771–793.

—, MATEUS, O., BUTLER, R., BRUSATTE, S. and WHITESIDE, J. 2011. A new metoposaurid (temnospondyl) bonebed from the Late Triassic of Portugal. *Journal of Vertebrate Paleontology*, **31** (Program and Abstracts), 200A.

SUES, H. D. and OLSEN, P. E. 2015. Stratigraphic and temporal context and faunal diversity of Permian-Jurassic continental tetrapod assemblages from the Fundy rift basin, eastern Canada. *Atlantic Geology*, **51**, 139–205.

SULEJ, T. 2002. Species discrimination of the Late Triassic temnospondyl amphibian *Metoposaurus diagnosticus. Acta Paleontologica Polonica*, **47** (3), 535–546.

— 2007. Osteology, variability and evolution of *Metoposaurus*, a temnospondyl from the Late Triassic of Poland. *Paleontologica Polonica*, **64**, 29–139.

SWOFFORD, D. L. 2003. PAUP*. Phylogenetic Analysis Using Parsimony (*and other Methods). Version 4. Sinauer, Sunderland, Massachusetts, USA.

SZULC, J. 2005. Sedimentary environments of the vertebrate-bearing Norian deposits from Krasiejów, Upper Silesia (Poland). *Hallesches Jahrbuch für geowissenschaften Reihe B*, **19**, 161–170.

—, RACKI, G., JEWUŁA, K. and ŚRODOŃ, J. 2015. How many Upper Triassic bone-bearing levels are there in Upper Silesia (southern Poland)? A critical overview of stratigraphy and facies. *Annales Societatis Geologorum Poloniae*, **85** (4), 587–626.

TOURANI, A., LUND, J. J., BENAOUISS, N. and GAUPP, R. 2000. Stratigraphy of Triassic syn-rift deposition in Western Morocco. *Zentralblatt für Geologie und Paläontologie*, **9** (10), 1193–1215.

WATSON, D. M. S. 1919. The Structure, Evolution and Origin of the Amphibia. The Orders Rachitomi and Stereospondyli. *Philosophical Transactions of the Royal Society of London, Series B*, **209**, 73 pp.

WARREN, A.A. and MARSICANO, C.A. 2000. A phylogeny of the Brachyopoidea (Temnospondyli, Stereospondyli). *Journal of Vertebrate Paleontology*, **20**, 462–483.

—, DAMIANI, R. J. and YATES, A. 2000. Paleobiogeography of Australian Fossil Amphibians. *Historical Biology*, **15**, 171–179.

WILSON, J. A. 1948. A small amphibian from the Triassic of Howard County, Texas. *Journal of Paleontology*, **22** (3), 359–361.

YATES, A., and WARREN, A. A. 2000. The phylogeny of the 'higher' temnospondyls (Vertebrata: Choanata) and its implications for the monophyly and origins of the Stereospondyli. *Zoological Journal of the Linnean Society*, **128**, 77–121.

ZITTEL, K. A. von. 1888. *Handbuch der Paläeontologie. Abteilung 1. Paläeozoologie Band III. Vertebrata (Pisces, Amphibia, Reptilia, Aves)*. Oldenbourg, Berlin, 598 pp.

FIGURE CAPTIONS

FIG. 1. *Arganasaurus* (*Metoposaurus*) *azerouali* (Dutuit, 1976) comb. nov., from the Late Triassic of the Argana Basin, Morocco: MNHN.F.ARG 5, holotype skull in dorsal view. A, photograph; B, interpretive drawing. Scale bars represent 10 cm. *Anatomical abbreviations:* Fr, frontal; Ju, jugal; La, lacrimal; Mx, maxilla; Na, nasal; Orb, orbit; Pa, parietal; Pfr, postfrontal; Pif, pineal foramen; Po, postorbital; Po.c, postorbital canal; Ppa, postparietal; Prf, prefrontal; Qj, quadratojugal; So.c, supraorbital canal; Sq, squamosal; Su, supratemporal; Tab, tabular.

FIG. 2. *Arganasaurus* (*Metoposaurus*) *azerouali* (Dutuit, 1976) comb. nov., from the Late Triassic of the Argana Basin, Morocco: MNHN.F.TAL 12 and MNHN.F.TAL 17 skull fragments. A, MNHN.F.TAL 12 in dorsal view; B, MNHN.F.TAL 12 in ventral view; C, MNHN.F.TAL 17 in dorsal view. Scale bars represent 10 cm.

FIG. 3. *Arganasaurus* (*Metoposaurus*) *azerouali* (Dutuit, 1976) comb. nov., from the Late Triassic of the Argana Basin, Morocco: MNHN.F.ARG 5, holotype skull in ventral view. A, photograph; B, interpretive drawing. Scale bars represent 10 cm. *Anatomical abbreviations:* Ch, choana; Cr.ms, crista muscularis; Cu.pr, cultriform process of the parasphenoid; Ect, ectopterygoid; Exo, exoccipital; If, interpterygoid fenestra; Orb, orbit; Pal, palatine; Pal.t, palatal tusk; Ps, parasphenoid; Pt, pterygoid; Q, quadrate; Stf, subtemporal fenestra; Vo, vomer.

FIG. 4. *Arganasaurus* (*Metoposaurus*) *azerouali* (Dutuit, 1976) comb. nov., from the Late Triassic of the Argana Basin, Morocco: MNHN.F.ARG 5, holotype skull in occipital view. A, photograph; B, interpretive drawing. Scale bars represent 10 cm. *Anatomical abbreviations:* Cr.fal, crista falciformis; Exo, exoccipital; Fm, foramen magnum; Oc, occipital condyle; Of, otic flange; On, otic notch; Ppa, postparietal; Pq.f, paraquadrate foramen; Pt, pterygoid; Pt.f, posttemporal foramen; Q, quadrate; Qj, quadratojugal; Sq, squamosal; Tab, tabular.

FIG. 5. *Arganasaurus* (*Metoposaurus*) *azerouali* (Dutuit, 1976) comb. nov., from the Late Triassic of the Argana Basin, Morocco: MNHN.F.ARG 3. Complete right hemi-mandible in labial view, A, photograph; B, interpretive drawing; and lingual view, C, photograph; D, interpretive drawing. Scale bars represent 10 cm. *Anatomical abbreviations:* Am.c, accessory mandibular canal; aMf, anterior Meckelian fenestra; Ang, angular; Art, articular; Co1, anterior coronoid; Co2, intercoronoid; Co3, posterior coronoid; De, dentary; Glf, glenoid fossa; Im.c, inferior mandibular canal; Par, prearticular; poGl.Pr, postglenoid process; pMf, posterior Mekelian fenestra; poSp, postsplenial; prGl.Pr, preglenoid process; Rart.Pr, retroarticular process; Sang, surangular; Sm.c, superior mandibular canal; Sp, splenial; Sy, symphysis.

FIG. 6. *Arganasaurus* (*Metoposaurus*) *azerouali* (Dutuit, 1976) comb. nov., from the Late Triassic of the Argana Basin, Morocco: MNHN.F.ARG9-1-3, paratype, articulated clavicles MNHN.F.ARG 9.1 and MNHN.F.ARG 9.2 and interclavicle MNHN.F.ARG 9.3 in ventral view. A, photograph; B, interpretive drawing. Scale bars represent 15 cm. *Anatomical abbreviations:* Cl, clavicle; Cl.c, clavicular canal; Ic, interclavicle.

FIG. 7. *Arganasaurus* (*Metoposaurus*) *azerouali* (Dutuit, 1976) comb. nov., from the Late Triassic of the Argana Basin, Morocco: MNHN.F.TAL 12, isolated radius encased in the ventral surface of the skull fragment. *Anatomical abbreviations:* Orb, orbit; Ra, radius.

FIG. 8. Phylogeny of the Metoposauroidea and position of *Arganasaurus* (*Metoposaurus*) *azerouali* (Dutuit, 1976) comb. nov.. Strict consensus of three most parsimonious trees (L=143; CI = 0.5385; RI = 0.6118, see text) mapped on the stratigraphic chart of the Middle and Late Triassic (stratigraphic chart after Cohen *et al.* 2018). Node labels: Node letter/Bremer support value (when above 1). Black bars indicate the unambiguous stratigraphic distribution of the taxa and dotted lines indicate the range of uncertainty of this distribution. CPE scale bar represents the duration of the Carnian Pluvial Episode (dated according to Dal Corso *et al.*

2018). *Abbreviations:* Myr, million years. Carn., Carnian; Hett., Hettangian; Ladin., Ladinian; Rhaet., Rhaetian; Sinem., Sinemurian.

FIG. 9. Correlation chart of all the Late Triassic metoposauroid-bearing formations across Pangaea. Stratigraphic chart after Cohen *et al.* (2018), uncertainty on the duration of the Norian stage collowing Ogg *et al*. (2014), Land Vertebrate Faunachrons (LVF) according to Lucas (2018b) and Carnian Pluvial Episode (CPE, in blue) dated according to Dal Corso *et al.* (2018). Dotted lines indicate an uncertain age and arrows indicate the extent of this uncertainty. Abbreviations: Adam., Adamanian; Alaun., Alaunian; Apach., Apachean; Berdyan., Berdyankian; Fass., Fassanian; Fm., Formation; Longob., Longobardian; Mb., Member; Otisch., Otischalkian; Perov., Perovkan; Revuel., Revueltian; Sevat., Sevatian; Tuval., Tuvalian; Wass., Wassonian.

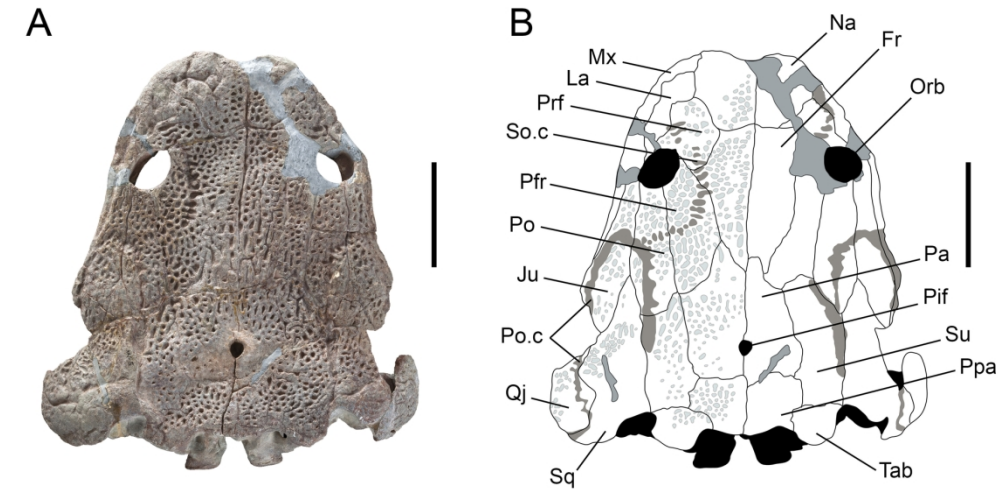

FIG. 1. Arganasaurus (Metoposaurus) azerouali (Dutuit, 1976) comb. nov., from the Late Triassic of the Argana Basin, Morocco: MNHN.F.ARG 5, holotype skull in dorsal view. A, photograph; B, interpretive drawing. Scale bars represent 10 cm. Anatomical abbreviations: Fr, frontal; Ju, jugal; La, lacrimal; Mx, maxilla; Na, nasal; Orb, orbit; Pa, parietal; Pfr, postfrontal; Pif, pineal foramen; Po, postorbital; Po.c, postorbital canal; Ppa, postparietal; Prf, prefrontal; Qj, quadratojugal; So.c, supraorbital canal; Sq, squamosal; Su, supratemporal; Tab, tabular.

165x86mm (300 x 300 DPI)

FIG. 2. Arganasaurus (Metoposaurus) azerouali (Dutuit, 1976) comb. nov., from the Late Triassic of the Argana Basin, Morocco: MNHN.F.TAL 12 and MNHN.F.TAL 17 skull fragments. A, MNHN.F.TAL 12 in dorsal view; B, MNHN.F.TAL 12 in ventral view; C, MNHN.F.TAL 17 in dorsal view. Scale bars represent 10 cm.

165x94mm (300 x 300 DPI)

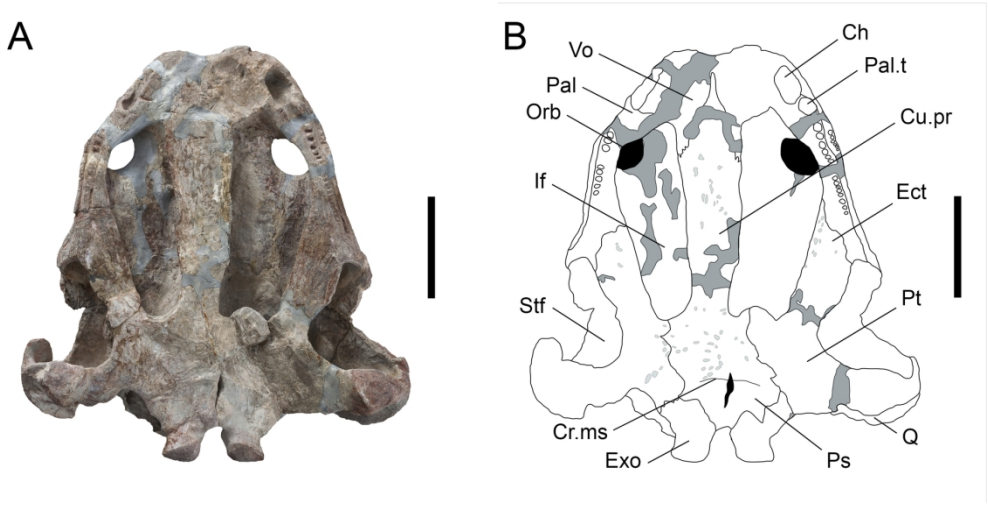

FIG. 3. Arganasaurus (Metoposaurus) azerouali (Dutuit, 1976) comb. nov., from the Late Triassic of the Argana Basin, Morocco: MNHN.F.ARG 5, holotype skull in ventral view. A, photograph; B, interpretive drawing. Scale bars represent 10 cm. Anatomical abbreviations: Ch, choana; Cr.ms, crista muscularis; Cu.pr, cultriform process of the parasphenoid; Ect, ectopterygoid; Exo, exoccipital; If, interpterygoid fenestra; Orb, orbit; Pal, palatine; Pal.t, palatal tusk; Ps, parasphenoid; Pt, pterygoid; Q, quadrate; Stf, subtemporal fenestra; Vo, vomer.

166x83mm (300 x 300 DPI)

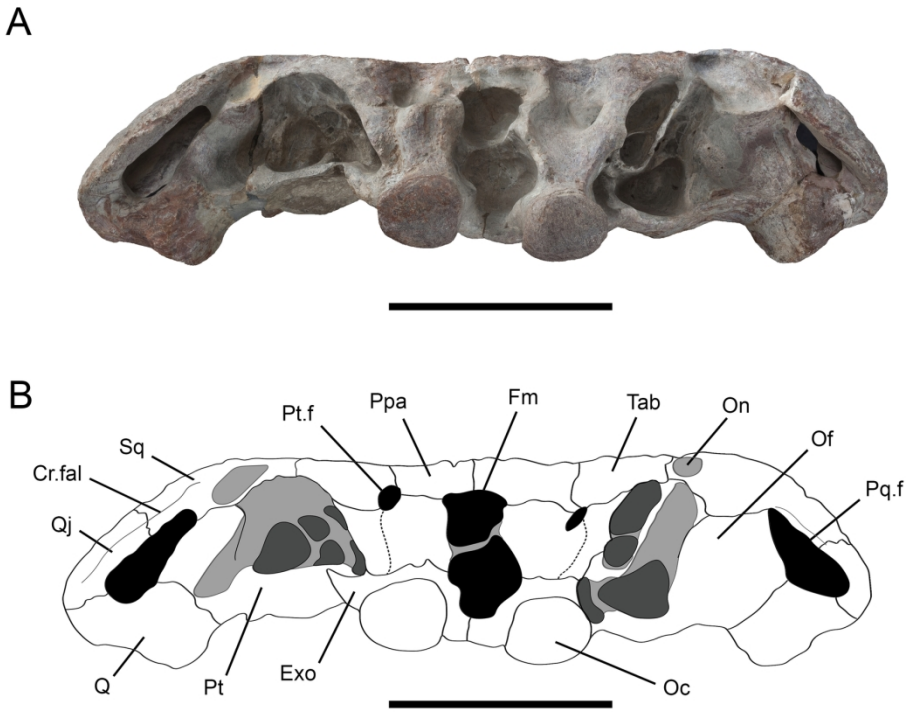

FIG. 4. Arganasaurus (Metoposaurus) azerouali (Dutuit, 1976) comb. nov., from the Late Triassic of the Argana Basin, Morocco: MNHN.F.ARG 5, holotype skull in occipital view. A, photograph; B, interpretive drawing. Scale bars represent 10 cm. Anatomical abbreviations: Cr.fal, crista falciformis; Exo, exoccipital; Fm, foramen magnum; Oc, occipital condyle; Of, otic flange; On, otic notch; Ppa, postparietal; Pq.f, paraquadrate foramen; Pt, pterygoid; Pt.f, posttemporal foramen; Q, quadrate; Qj, quadratojugal; Sq, squamosal; Tab, tabular.

165x125mm (300 x 300 DPI)

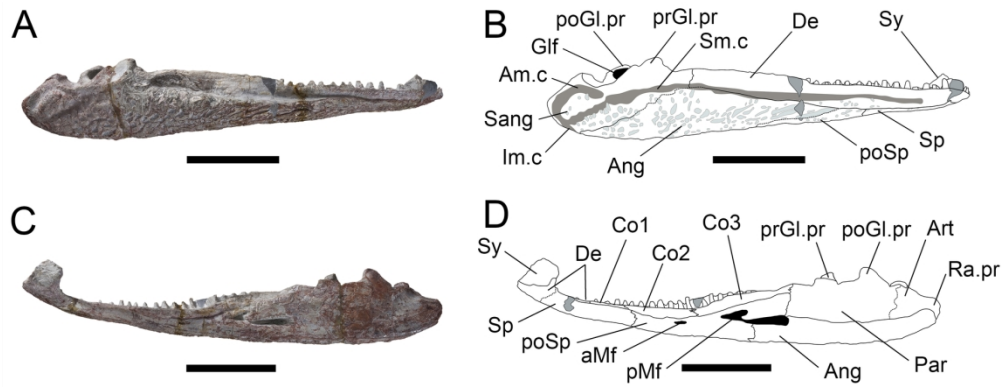

FIG. 5. Arganasaurus (Metoposaurus) azerouali (Dutuit, 1976) comb. nov., from the Late Triassic of the Argana Basin, Morocco: MNHN.F.ARG 3. Complete right hemi-mandible in labial view, A, photograph; B, interpretive drawing; and lingual view, C, photograph; D, interpretive drawing. Scale bars represent 10 cm. Anatomical abbreviations: Am.c, accessory mandibular canal; aMf, anterior Meckelian fenestra; Ang, angular; Art, articular; Co1, anterior coronoid; Co2, intercoronoid; Co3, posterior coronoid; De, dentary; Glf, glenoid fossa; Im.c, inferior mandibular canal; Par, prearticular; poGl.Pr, postglenoid process; pMf, posterior Mekelian fenestra; poSp, postsplenial; prGl.Pr, preglenoid process; Rart.Pr, retroarticular process; Sang, surangular; Sm.c, superior mandibular canal; Sp, splenial; Sy, symphysis.

165x63mm (300 x 300 DPI)

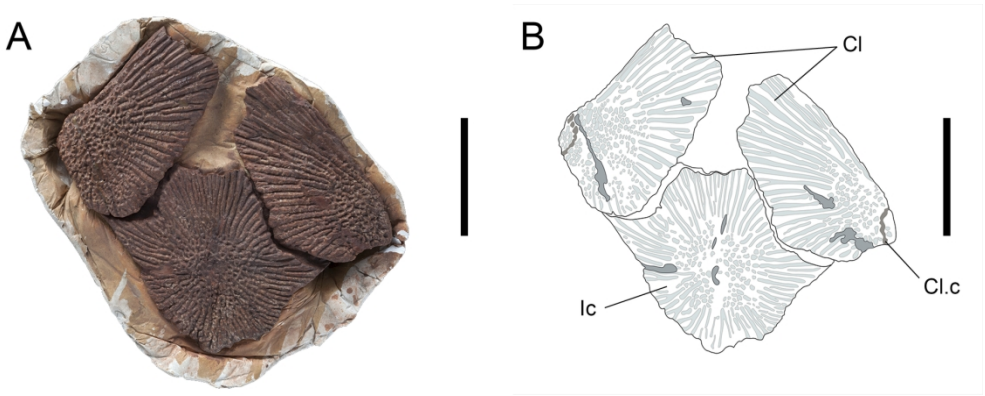

FIG. 6. Arganasaurus (Metoposaurus) azerouali (Dutuit, 1976) comb. nov., from the Late Triassic of the Argana Basin, Morocco: MNHN.F.ARG9-1-3, paratype, articulated clavicles MNHN.F.ARG 9.1 and MNHN.F.ARG 9.2 and interclavicle MNHN.F.ARG 9.3 in ventral view. A, photograph; B, interpretive drawing. Scale bars represent 15 cm. Anatomical abbreviations: Cl, clavicle; Cl.c, clavicular canal; Ic, interclavicle.

166x64mm (300 x 300 DPI)

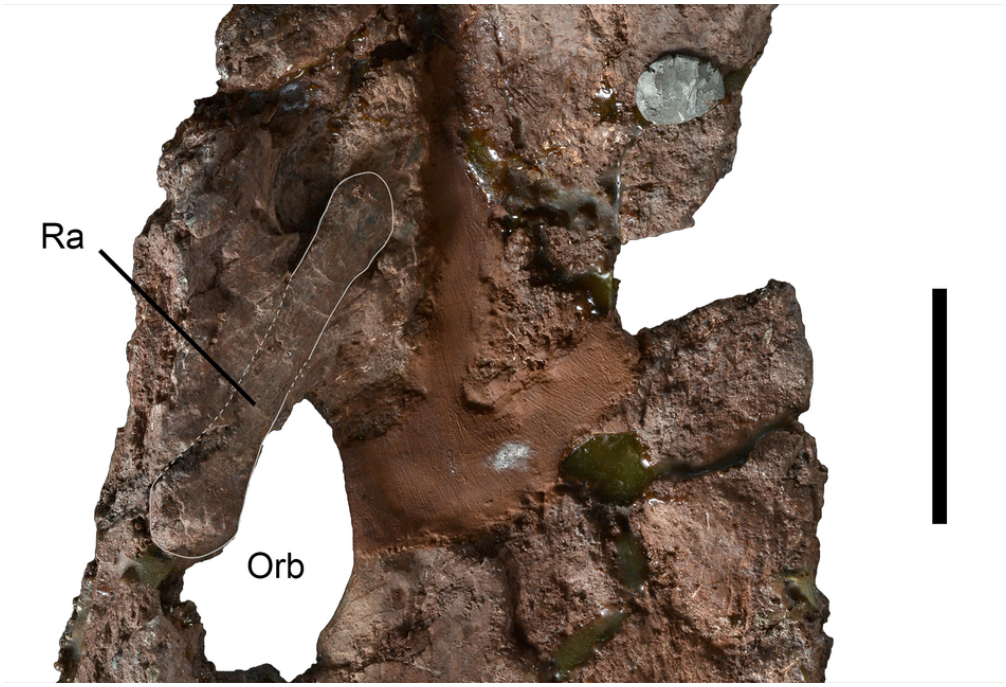

FIG. 7. Arganasaurus (Metoposaurus) azerouali (Dutuit, 1976) comb. nov., from the Late Triassic of the Argana Basin, Morocco: MNHN.F.TAL 12, isolated radius encased in the ventral surface of the skull fragment. Anatomical abbreviations: Orb, orbit; Ra, radius.

80x54mm (300 x 300 DPI)

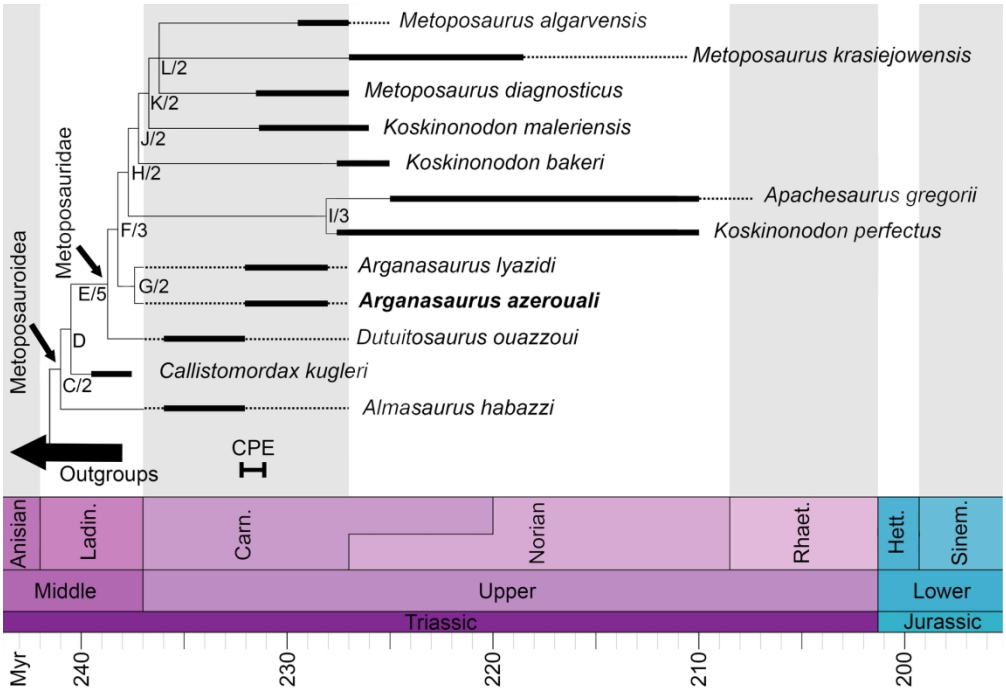

FIG. 8. Phylogeny of the Metoposauroidea and position of Arganasaurus (Metoposaurus) azerouali (Dutuit, 1976) comb. nov.. Strict consensus of three most parsimonious trees (L=143; CI = 0.5385; RI = 0.6118, see text) mapped on the stratigraphic chart of the Middle and Late Triassic (stratigraphic chart after Cohen et al. 2018). Node labels: Node letter/Bremer support value (when above 1). Black bars indicate the unambiguous stratigraphic distribution of the taxa and dotted lines indicate the range of uncertainty of this distribution. CPE scale bar represents the duration of the Carnian Pluvial Episode (dated according to Dal Corso et al. 2018). Abbreviations: Myr, million years. Carn., Carnian; Hett., Hettangian; Ladin., Ladinian; Rhaet., Rhaetian; Sinem., Sinemurian.

165x114mm (300 x 300 DPI)

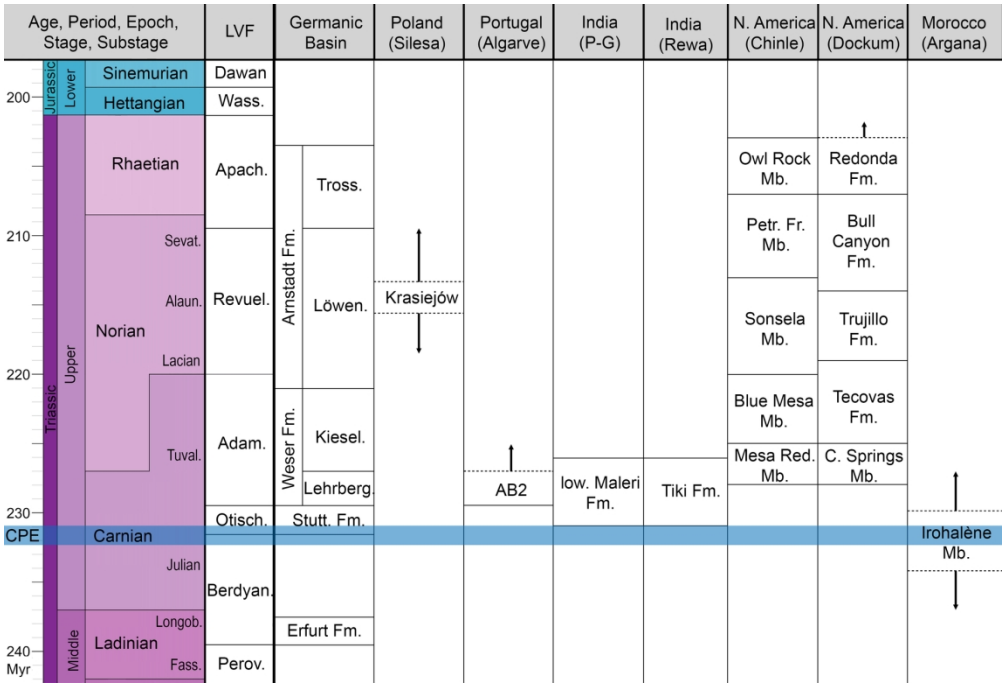

FIG. 9. Correlation chart of all the Late Triassic metoposauroid-bearing formations across Pangaea. Stratigraphic chart after Cohen et al. (2018), uncertainty on the duration of the Norian stage collowing Ogg et al. (2014), Land Vertebrate Faunachrons (LVF) according to Lucas (2018b) and Carnian Pluvial Episode (CPE, in blue) dated according to Dal Corso et al. (2018). Dotted lines indicate an uncertain age and arrows indicate the extent of this uncertainty. Abbreviations: Adam., Adamanian; Alaun., Alaunian; Apach., Apachean; Berdyan., Berdyankian; Fass., Fassanian; Fm., Formation; Longob., Longobardian; Mb., Member; Otisch., Otischalkian; Perov., Perovkan; Revuel., Revueltian; Sevat., Sevatian; Tuval., Tuvalian; Wass., Wassonian.

165x112mm (300 x 300 DPI)